

---

## CHAPTER 12

---

---

# INTRODUCTION TO MOTOR DRIVES

---

### 12-1 INTRODUCTION

Motor drives are used in a very wide power range, from a few watts to many thousands of kilowatts, in applications ranging from very precise, high-performance position-controlled drives in robotics to variable-speed drives for adjusting flow rates in pumps. In all drives where the speed and position are controlled, a power electronic converter is needed as an interface between the input power and the motor.

Above a few hundred watt power level, there are basically the following three types of motor drives, which are discussed in Chapters 13 through 15: (1) dc motor drives, (2) induction motor drives, and (3) synchronous motor drives.

A general block diagram for the control of motor drives is shown in Fig. 12-1. The process determines the requirements on the motor drive; for example, a servo-quality drive (called the servo drive) is needed in robotics, whereas only an adjustable-speed drive may be required in an air conditioning system, as explained further.

In servo applications of motor drives, the response time and the accuracy with which the motor follows the speed and position commands are extremely important. These servo systems, using one of these motor drives, require speed or position feedback for a precise control, as shown in Fig. 12-2. In addition, if an ac motor drive is used, the controller must incorporate sophistication, such as field-oriented control, to make the ac motor (through the power electronic converter) meet the servo drive requirements.

However, in a large number of applications, the accuracy and the response time of the motor to follow the speed command is not critical. As shown in Fig. 12-1, there is a

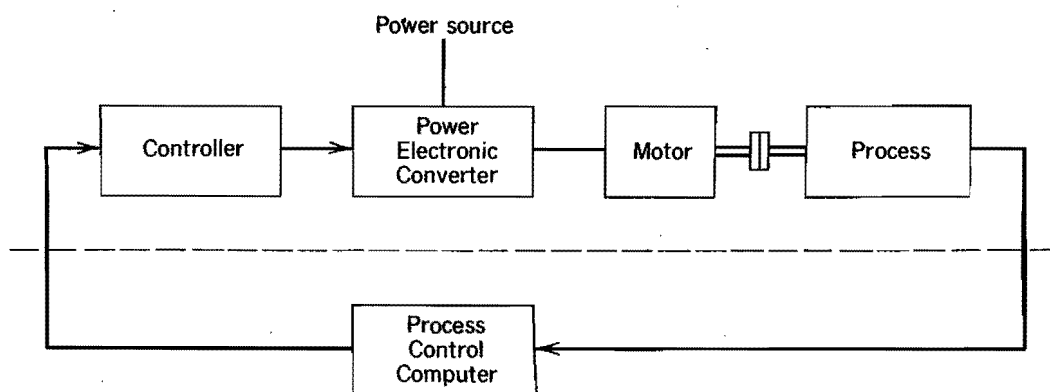


Figure 12-1 Control of motor drives.

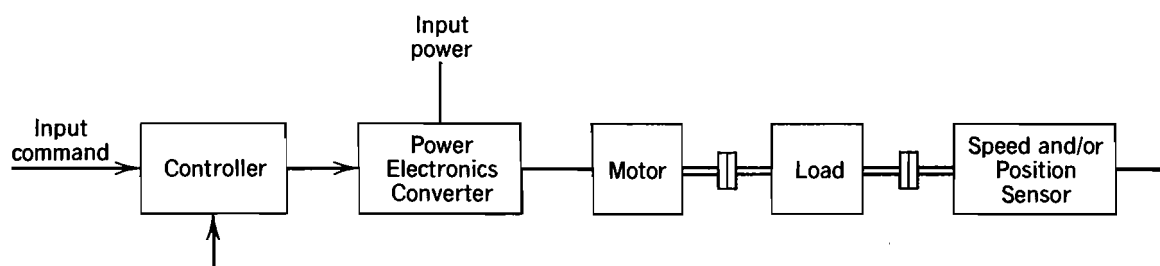


Figure 12-2 Servo drives.

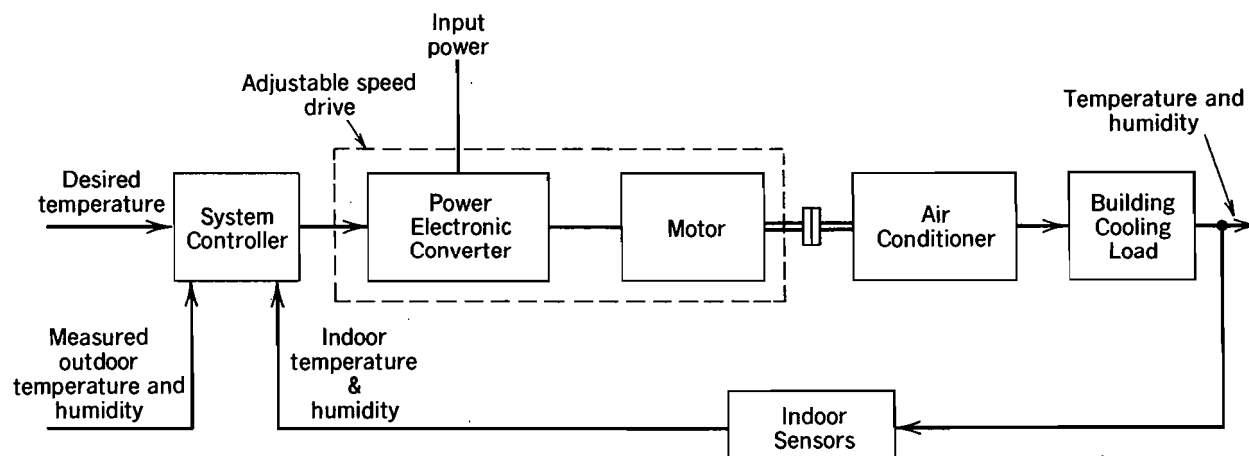


Figure 12-3 Adjustable-speed drive in an air conditioning system.

feedback loop to control the process, outside of the motor drive. Because of the large time constants associated with the process-control feedback loop, the motor drive's accuracy and the time of response to speed commands are not critical. An example of such an adjustable-speed drive is shown in Fig. 12-3 for an air conditioning system.

## 12-2 CRITERIA FOR SELECTING DRIVE COMPONENTS

As shown in Figs. 12-1 through 12-3, a motor drive consists of an electric motor, a power electronic converter, and possibly a speed and/or position sensor. In this section, criteria for optimum match between the mechanical load and the drive components are discussed in general terms.

### 12-2-1 MATCH BETWEEN THE MOTOR AND THE LOAD

Prior to selecting the drive components, the load parameters and requirements such as the load inertia, maximum speed, speed range, and direction of motion must be available. The motion profile as a function of time, for example as shown in Fig. 12-4a, must also be specified. By means of modeling the mechanical system, it is possible to obtain a load-torque profile. Assuming a primarily inertial load with a negligible damping, the torque profile, corresponding to the speed profile in Fig. 12-4a, is shown in Fig. 12-4b. The torque required by the load peaks during the acceleration and deceleration.

One way to drive a rotating load is to couple it directly to the motor. In such a direct coupling, the problems and the losses associated with a gearing mechanism are avoided. But the motor must be able to provide peak torques at specified speeds. The other option for a rotating load is to use a gearing mechanism. A coupling mechanism such as rack-

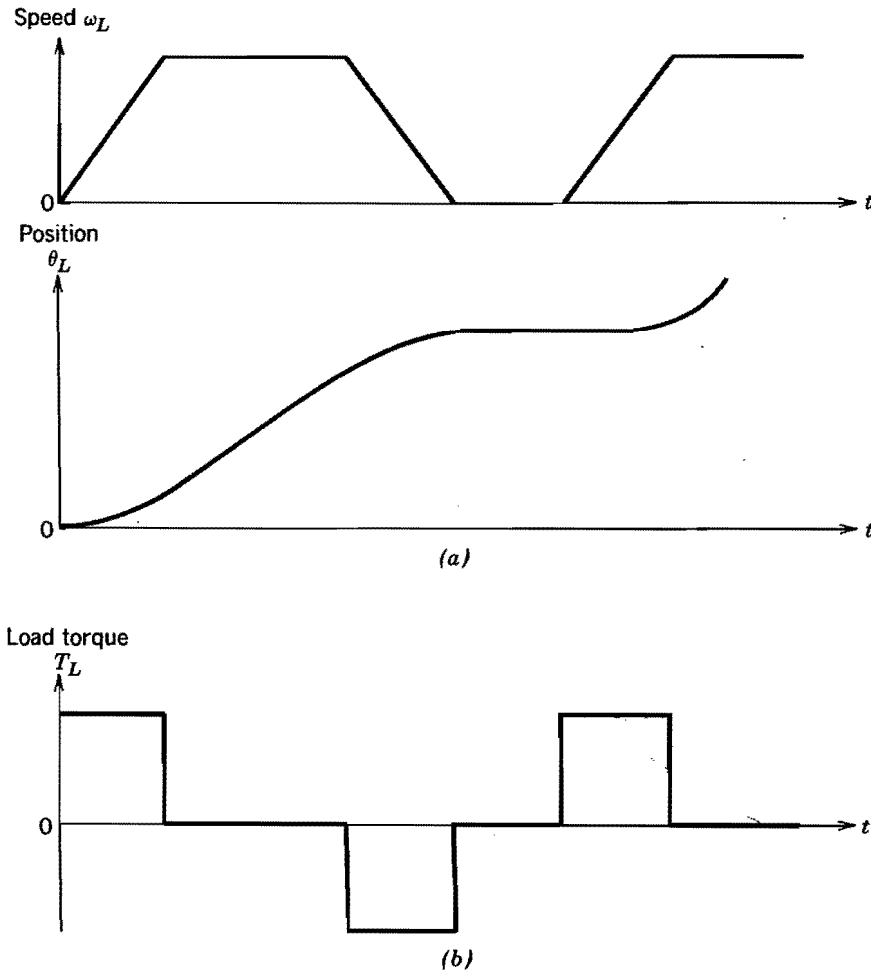


**Figure 12-4** Load profile: (a) load-motion profile; (b) load-torque profile (assuming a purely inertial load).

and-pinion, belt-and-pulley, or feed-screw must be used to couple a load with a linear motion to a rotating motor. A gear and a feed-screw drive are shown in Figs. 12-5a and 12-5b, respectively. Assuming the energy efficiency of the gear in Fig. 12-5a to be 100%, the torques on the two sides of the gear are related as

$$\frac{T_m}{T_L} = \frac{\omega_L}{\omega_m} = \frac{\theta_L}{\theta_m} = \frac{n_m}{n_L} = a \quad (12-1)$$

where the angular speed  $\omega = \dot{\theta}$ ,  $n_m$  and  $n_L$  are the number of teeth, and  $a$  is the coupling ratio.

In the feed-screw drive of Fig. 12-5b, the torque and the force are related as

$$\frac{T_m}{F_L} = \frac{v_L}{\omega_m} = \frac{x_L}{\theta_m} = \frac{s}{2\pi} = a \quad (12-2)$$

where the linear velocity  $v_L = \dot{x}_L$ ,  $s$  is the pitch of the feed screw in  $m/\text{turn}$ , and  $a$  is the coupling ratio.

The electromagnetic torque  $T_{em}$  required from the motor can be calculated on the basis of energy considerations in terms of the inertias, required load acceleration, coupling ratio  $a$ , and the working torque or force. In Fig. 12-5a,  $T_{WL}$  is the working torque of the load and  $\dot{\omega}_L$  is the load acceleration. Therefore,

$$T_{em} = \frac{\dot{\omega}_L}{a} [J_m + a^2 J_L] + a T_{WL} + \frac{\omega_L}{a} (B_m + a^2 B_L) \quad (12-3a)$$

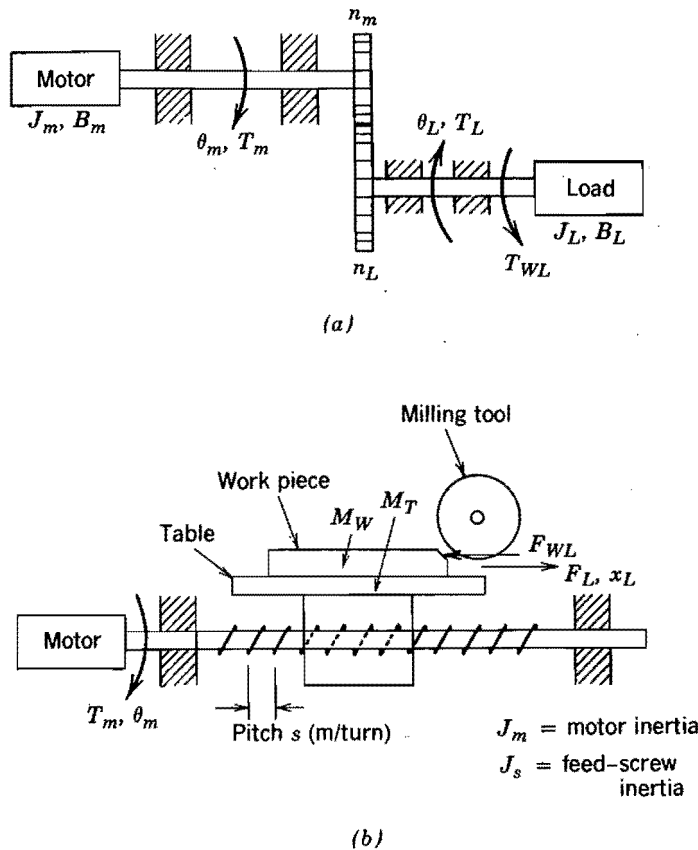


**Figure 12-5** Coupling mechanisms: (a) gear; (b) feed screw.

This equation can be written in terms of the motor speed (recognizing that  $\omega_m = \omega_L/a$ ), the equivalent total inertia  $J_{eq} = J_m + a^2 J_L$ , the equivalent total damping  $B_{eq} = B_m + a^2 B_L$ , and the equivalent working torque of the load  $T_{Weq} = aT_{WL}$ :

$$T_{em} = J_{eq} \dot{\omega}_m + B_{eq} \omega_m + T_{Weq} \quad (12-3b)$$

Similarly, for the feed-screw system in Fig. 12-5b with  $F_{WL}$  as the working or the machining force and  $a$  as the coupling ratio calculated in Eq. 12-2 in terms of pitch  $s$ ,  $T_{em}$  can be calculated as (see Problem 12-3)

$$T_{em} = \frac{\dot{v}_L}{a} [J_m + J_s + a^2(M_T + M_W)] + aF_{WL} \quad (12-4)$$

where  $\dot{v}_L$  is the linear acceleration of the load.

As indicated by Eqs. 12-1 and 12-2, the choice of the coupling ratio  $a$  affects the motor speed. At the same time, the value of  $a$  affects the peak electromagnetic torque  $T_{em}$  required from the motor, as is indicated by Eqs. 12-3a and 12-4. In selecting the optimum value of the coupling ratio  $a$ , the cost and losses associated with the coupling mechanism must also be included.

### 12-2-2 THERMAL CONSIDERATIONS IN SELECTING THE MOTOR

In the previous section, the match between the load and the motor is discussed that establishes the peak torque and the maximum speed required from the motor. This matching also establishes the motor-torque profile, which, for example, has the same form (but different magnitudes) as the load-torque profile of Fig. 12-4b.

As another example, the electromagnetic torque required from the motor as a function of time is obtained as shown in Fig. 12-6a. In electric machines, the electromagnetic

torque produced by the motor is proportional to the motor current  $i$ , provided the flux in the air gap of the motor is kept constant. Therefore, the motor-current profile is identical to the motor-torque profile, as shown in Fig. 12-6b. The motor current in Fig. 12-6b during various time intervals is a dc current for a dc motor. For an ac motor, the motor current shown is approximately the rms value of the ac current drawn during various time intervals. The power loss  $P_R$  in the winding resistance  $R_M$  due to the motor current is a large part of the total motor losses, which get converted into heat. This resistive loss is proportional to the square of the motor current and, hence, proportional to  $T_{em}^2$  during various time intervals in Figs. 12-6a and 12-6b. If the time period  $t_{\text{period}}$  in Fig. 12-6, with which the waveforms repeat, is short compared with the motor thermal time constant, then the motor heating and the maximum temperature rise can be calculated based on the resistive power loss  $P_R$  averaged over the time period  $t_{\text{period}}$ . Therefore, in Fig. 12-6, the rms value of the current over the period of repetition can be obtained as

$$P_R = R_M I_{\text{rms}}^2 \quad (12-5)$$

where

$$I_{\text{rms}}^2 = \frac{\sum_{k=1}^m I_k^2 t_k}{t_{\text{period}}} \quad (12-6)$$

and  $m = 6$  in this example.

Because of the motor current being linearly proportional to the motor torque, the rms value of the motor torque over  $t_{\text{period}}$  from Fig. 12-6 and Eq. 12-6 is

$$T_{\text{em, rms}}^2 = k_1 \frac{\sum_{k=1}^m I_k^2 t_k}{t_{\text{period}}} \quad (12-7)$$

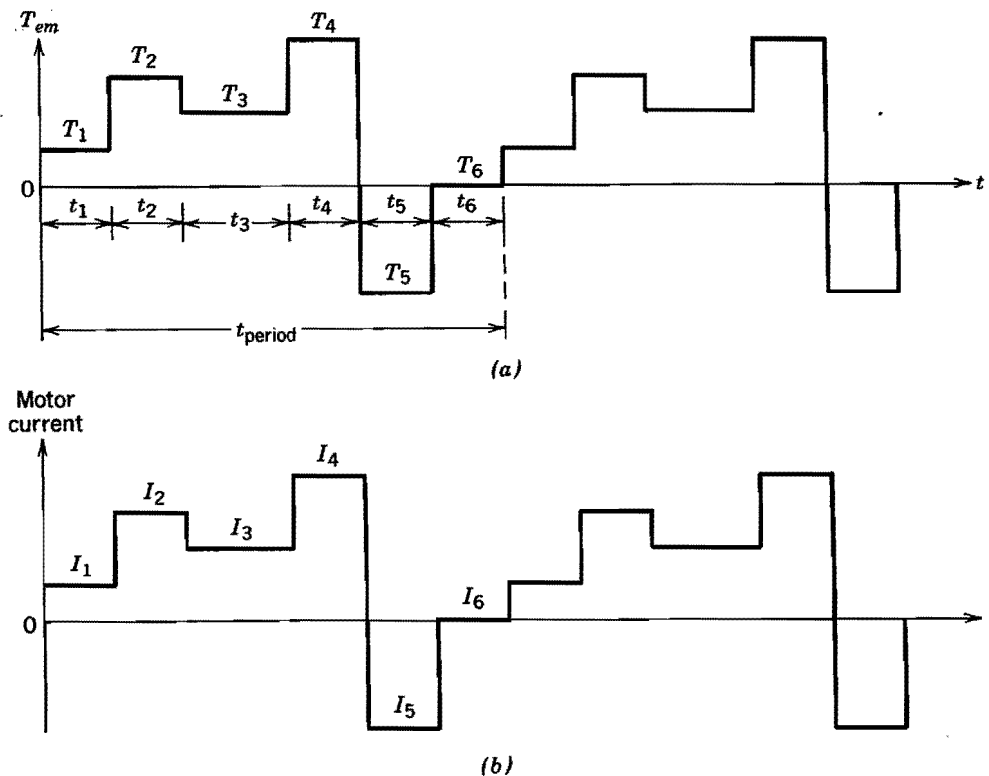


Figure 12-6 Motor torque and current.

and therefore,

$$T_{\text{em, rms}}^2 = k_1 I_{\text{rms}}^2 \quad (12-8)$$

where  $k_1$  is a constant of proportionality.

From Eqs. 12-5 and 12-8, the average resistive power loss  $P_R$  is given as

$$P_R = k_2 T_{\text{em, rms}}^2 \quad (12-9)$$

where  $k_2$  is a constant of proportionality.

In addition to  $P_R$ , there are other losses within the motor that contribute to its heating. These are  $P_{\text{FW}}$  due to friction and windage,  $P_{\text{EH}}$  due to eddy currents and hysteresis within the motor laminations, and  $P_s$  due to switching frequency ripple in the motor current, since it is supplied by a switching power electronic converter rather than an ideal source. There are always some power losses called stray power losses  $P_{\text{stray}}$  that are not included with the foregoing losses. Therefore, the total power loss within the motor is

$$P_{\text{loss}} = P_R + P_{\text{FW}} + P_{\text{EH}} + P_s + P_{\text{stray}} \quad (12-10)$$

Under a steady-state condition, the motor temperature rise  $\Delta\Theta$  in degrees centigrade is given as

$$\Delta\Theta = P_{\text{loss}} R_{\text{TH}} \quad (12-11)$$

where  $P_{\text{loss}}$  is in watts and the thermal resistance  $R_{\text{TH}}$  of the motor is in degrees centigrade per watt.

For a maximum allowable temperature rise  $\Delta\Theta$ , the maximum permissible value of  $P_{\text{loss}}$  in steady state depends on the thermal resistance  $R_{\text{TH}}$  in Eq. 12-11. In general, the loss components other than  $P_R$  in the right side of Eq. 12-10 increase with the motor speed. Therefore, the maximum allowable  $P_R$  and, hence, the maximum continuous motor torque output from Eq. 12-9 would decrease at higher speed, if  $R_{\text{TH}}$  remains constant. However, in self-cooled motors with the fan connected to the motor shaft, for example,  $R_{\text{TH}}$  decreases at higher speeds due to increased air circulation at higher motor speeds. Therefore, the maximum safe operating area in terms of the maximum rms torque available from a motor at various speeds depends on the motor design and is specified in the motor data sheets (specially in case of servo motors). For a motor torque profile like that shown in Fig. 12-6a, the motor should be chosen such that the rms value of the torque required from the motor remains within the motor's safe operating area in the speed range of operation.

### 12-2-3 MATCH BETWEEN THE MOTOR AND THE POWER ELECTRONIC CONVERTER

A match between the load and the various characteristics of the motor, such as its inertia and the peak and the rms torque capability, have been discussed in the previous two sections. Depending on the power rating, speed of operation, operating environment, reliability, various other performance requirements by the load, and the cost of the overall drive, one of the following three types of motor drive is selected: dc motor drive, induction motor drive, and synchronous motor drive. The advantages and the disadvantages associated with each of these motor drives are discussed in Chapters 13 through 15.

The power electronic converter topology and its control depend on the type of motor drive selected. In general, the power electronic converter provides a controlled voltage to the motor in order to control the motor current and, hence, the electromagnetic torque produced by the motor. Some of the considerations in matching the power electronic converter to the motor are discussed in the following sections.

### 12-2-3-1 Current Rating

As we discussed previously, the rms value of the torque that a motor can supply depends on its thermal characteristics. However, a motor can supply substantially larger peak torques (as much as four times the continuous maximum torque) provided that the duration of the peak torque is small compared with the thermal time constant of the motor. Since  $T_{em}$  is proportional to  $i$ , a peak torque requires a corresponding peak current from the power electronic converter. The current capability of the power semiconductor devices used in the converter is limited by the maximum junction temperature within the devices and other considerations. A higher current results in a higher junction temperature due to power losses within the power semiconductor device. The thermal time constants associated with the power semiconductor devices are in general much smaller than the thermal time constants of various motors. Therefore, the current rating of the power electronic converter must be selected based on both the rms and the peak values of the torque that the motor is required to supply.

### 12-2-3-2 Voltage Rating

In both dc and ac motors, the motor produces a counter-emf  $e$  that opposes the voltage  $v$  applied to it, as shown by a simplified generic circuit of Fig. 12-7. The rate at which the motor current and, hence, the torque can be controlled is given by

$$\frac{di}{dt} = \frac{v - e}{L} \quad (12-12)$$

where  $L$  is the inductance presented by the motor to the converter.

To be able to quickly control the motor current and, hence, its torque, the output voltage  $v$  of the power electronic converter must be reasonably greater than the counter-emf  $e$ . The magnitude of  $e$  in a motor increases linearly with the motor speed, with a constant flux in the air gap of the motor. Therefore, the voltage rating of the power electronic converter depends on the maximum motor speed with a constant air-gap flux.

### 12-2-3-3 Switching Frequency and the Motor Inductance

In a servo drive, the motor current should be able to respond quickly to the load demand, thus requiring  $L$  to be small in Eq. 12-12. Also, the steady-state ripple in the motor current should be as small as possible to minimize the motor loss  $P_s$  in Eq. 12-10 and the ripple in the motor torque. A small current ripple requires the motor inductance  $L$  in Eq. 12-12 to be large. Because of the conflicting requirements on the value of  $L$ , the ripple in the motor current can be reduced by increasing the converter switching frequency. However, the switching losses in the power electronic converter increase linearly with the switching frequency. Therefore, a reasonable compromise must be made in selecting the motor inductance  $L$  and the switching frequency.

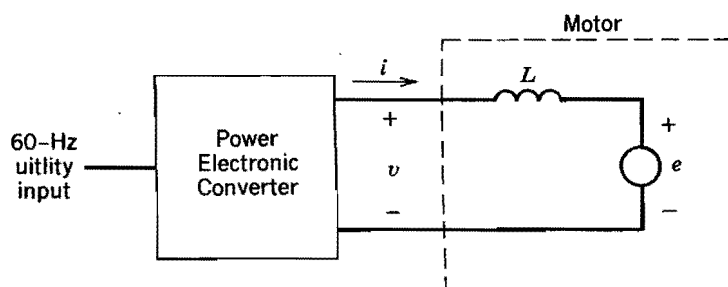


Figure 12-7 Simplified circuit of a motor drive.

### 12-2-4 SELECTION OF SPEED AND POSITION SENSORS

In selecting the speed and position sensors, the following items must be considered: direct or indirect coupling, sensor inertia, possibility and avoidance of torsional resonance, and the maximum sensor speed.

To control the instantaneous speed within a specified range, the ripple in the speed sensor should be small. This can be understood in terms of incremental position encoders, which are often used for measuring speed as well as position. If such a sensor is used at very low speeds, the number of pulse outputs per revolution must be large to provide instantaneous speed measurement with sufficient accuracy. Similarly, an accurate position information will require an incremental position encoder with a large number of pulse outputs per revolution.

### 12-2-5 SERVO DRIVE CONTROL AND CURRENT LIMITING

A block diagram of a servo drive was shown in Fig. 12-2. In most practical applications, a very fast response to a sudden change in position or speed command would require a large peak torque, which would result in a large peak current. This may be prohibitive in terms of the cost of the converter. Therefore, the converter current (same as the motor current) is limited by the controller. Figures 12-8a and 12-8b show two ways of implementing the current limit.

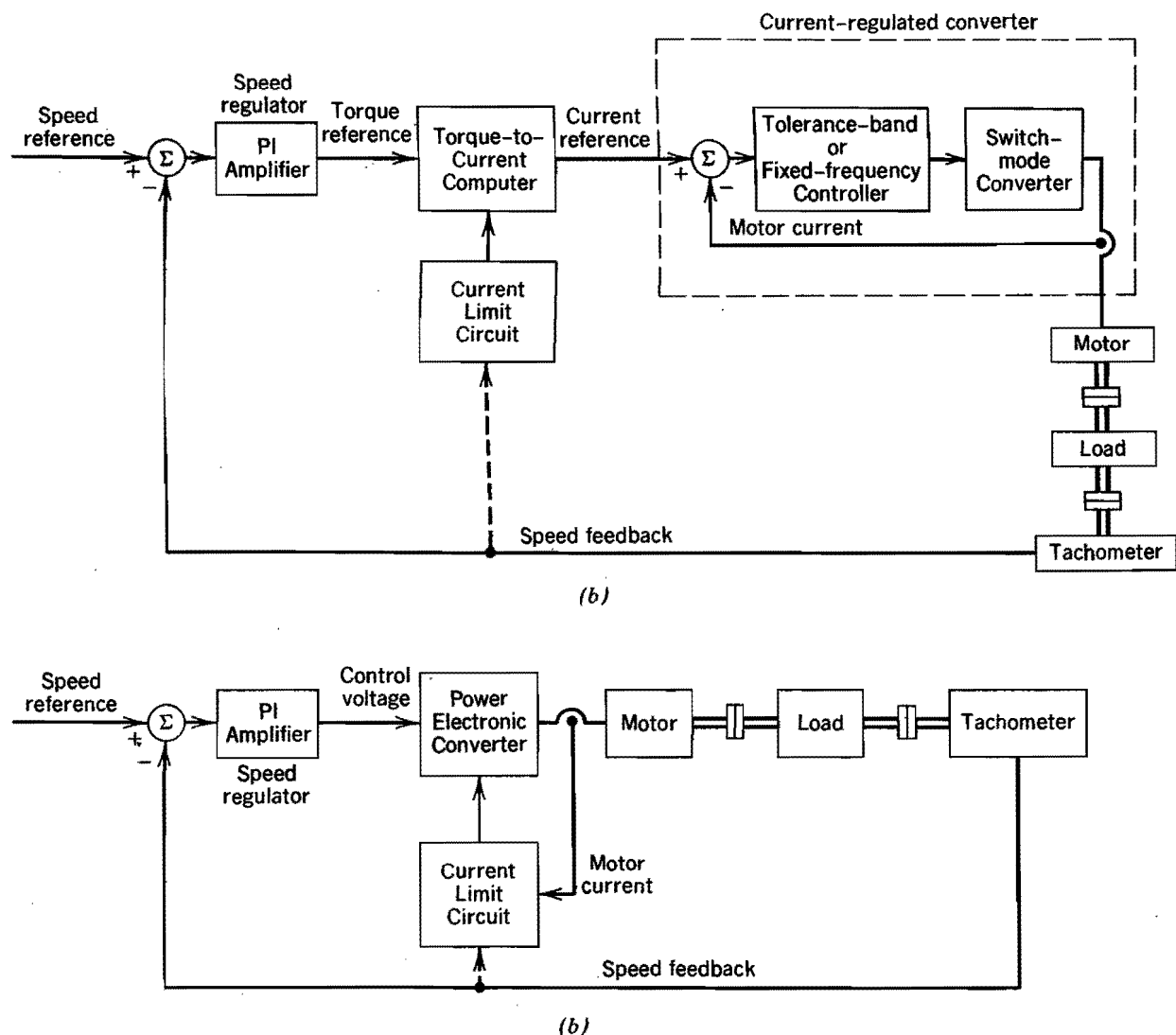


Figure 12-8 Control of servo drives: (a) inner current loop; (b) no inner current loop.



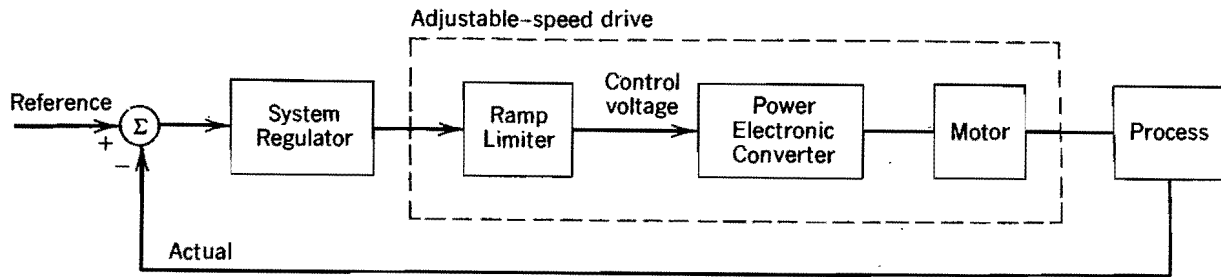


Figure 12-9 Ramp limiter to limit motor current.

In Fig. 12-8a, an inner current loop is used where the actual current is measured, and the error between the reference and the actual current controls the converter output current by means of a current-regulated modulation similar to that discussed in Section 8-6-3. Here, the power electronic converter operates as a current-regulated voltage source converter. An inner control loop improves the response time of the drive. As shown, the limit on the reference current may be dependent on the speed.

In the other control scheme shown in Fig. 12-8b, the error between the speed reference and the actual speed controls the converter through a proportional-integral (PI) amplifier. The output of the PI amplifier, which controls the converter, is suppressed only if the converter current exceeds the current limit. The current limit can be made to be speed dependent.

In a position control system, the speed reference signal in Figs. 12-8a and 12-8b is obtained from the position regulator. The input to such a position regulator will be the error between the reference position and the actual position.

#### 12-2-6 CURRENT LIMITING IN ADJUSTABLE-SPEED DRIVES

In adjustable-speed drives such as that shown in Fig. 12-3, the current is kept from exceeding its limit by means of limiting the rate of change of control voltage with time in the block diagram of Fig. 12-9.

## SUMMARY

1. Primary types of motor drives are dc motor drives, induction motor drives and synchronous motor drives.
2. Most of the applications of motor drives belong to one of the two categories: servo drives or adjustable-speed drives. In servo drive applications, the response time and the accuracy with which the motor follows the speed and/or position commands are extremely important. In adjustable-speed drive applications, response time to changes in speed command is not as critical; in fact, in many applications, it is not necessary to control the speed accurately where the process feedback loop has large time constants, relative to the response time of the drive.
3. A modeling of the mechanical system is necessary to determine the dynamics of the overall system and to select the motor and the power electronic converter of the appropriate ratings.
4. Servo drives require speed and/or position sensors to close the feedback loop. It is possible to operate with or without an inner current feedback loop. In an adjustable-speed drive, the current is kept within its limit by limiting the rate of change of control voltage to the power electronic converter with time.

## PROBLEMS

- 12-1 In the system shown in Fig. 12-5a, the gear ratio  $n_L/n_m = 2$ ,  $J_L = 10 \text{ kg-m}^2$ , and  $J_m = 2.5 \text{ kg-m}^2$ . Damping can be neglected. For the load-speed profile in Fig. P12-1, draw the torque profile and the rms value of the electromagnetic torque required from the motor.

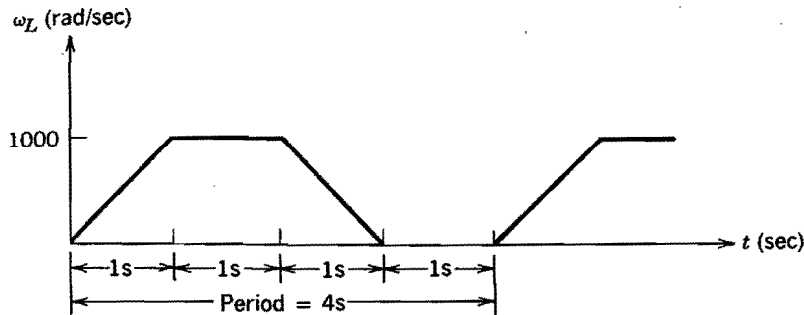


Figure P12-1

- 12-2 Consider the belt-and-pulley system shown in Fig. P12-2:

$J_m$  = motor inertia

$M$  = mass of load

$r$  = pulley radius

Other inertias are negligible.

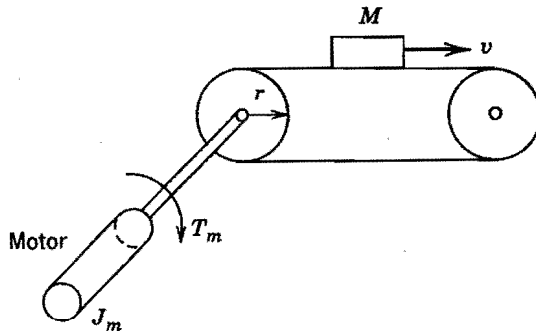


Figure P12-2

Calculate the torque  $T_{em}$  required from the motor to accelerate a load of 0.5 kg from rest to a velocity 1 m/s in a time of 3 s. Assume the motor torque to be constant during this interval, the pulley radius  $r = 0.1 \text{ m}$  and the motor inertia  $J_m = 0.006 \text{ kg-m}^2$ .

- 12-3 Derive Eq. 12-4.

- 12-4 In the system of Fig. 12-5a, assume a triangular velocity profile with equal acceleration and deceleration rates. The system is purely inertial and  $B_m$ ,  $B_L$ , and  $T_{wL}$  can be neglected.

Assuming a gear efficiency of 100% and an optimum gear ratio (such that the reflected load inertia equals the motor inertia), calculate the time needed to rotate the load by an angle  $\theta_L$  in terms of  $J_m$ ,  $J_L$ , and the peak torque  $T_{em}$  that the motor must be capable of developing.

## REFERENCES

1. H. Gross (Ed.), *Electrical Feed Drives for Machine Tools*, Siemens and Wiley, New York, 1983.
2. *DC Motors Speed Controls ServoSystem—An Engineering Handbook*, 5th ed., Electro-Craft Corporation, Hopkins, MN, 1980.
3. A. E. Fitzgerald, C. Kingsley, Jr., and S. D. Umans, *Electric Machinery*, 4th ed. McGraw-Hill, New York, 1983.
4. G. R. Slemon and A. Straughen, *Electric Machines*, Addison-Wesley, Reading, MA, 1980.

## CHAPTER 13

# dc MOTOR DRIVES

### 13-1 INTRODUCTION

Traditionally, dc motor drives have been used for speed and position control applications. In the past few years, the use of ac motor servo drives in these applications is increasing. In spite of that, in applications where an extremely low maintenance is not required, dc drives continue to be used because of their low initial cost and excellent drive performance.

### 13-2 EQUIVALENT CIRCUIT OF dc MOTORS

In a dc motor, the field flux  $\phi_f$  is established by the stator, either by means of permanent magnets as shown in Fig. 13-1a, where  $\phi_f$  stays constant, or by means of a field winding as shown in Fig. 13-1b, where the field current  $I_f$  controls  $\phi$ . If the magnetic saturation in the flux path can be neglected, then

$$\phi_f = k_f I_f \quad (13-1)$$

where  $k_f$  is a field constant of proportionality.

The rotor carries in its slots the so-called armature winding, which handles the electrical power. This is in contrast to most ac motors, where the power-handling winding is on the stator for ease of handling the larger amount of power. However, the armature winding in a dc machine has to be on the rotor to provide a “mechanical” rectification of voltages and currents (which alternate direction as the conductors rotate from the influence

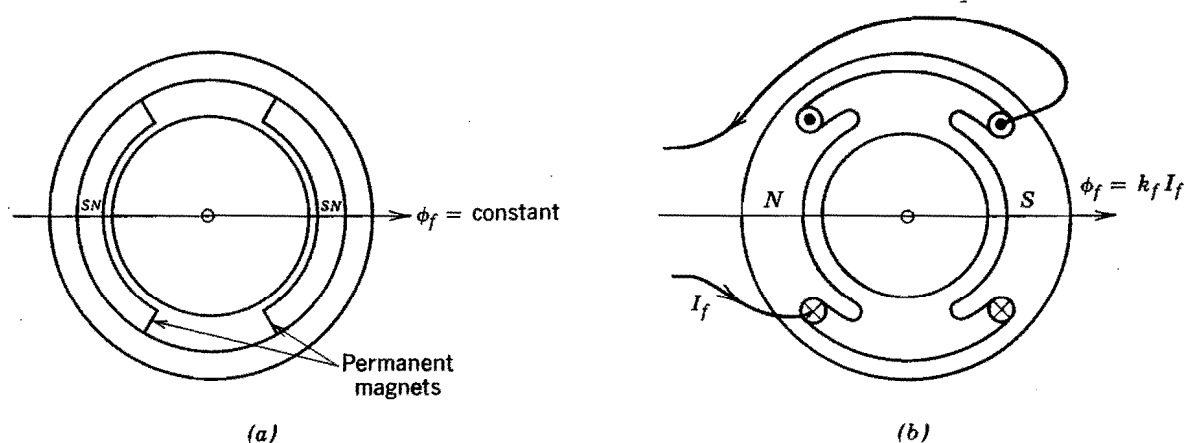


Figure 13-1 A dc motor: (a) permanent-magnet motor; (b) dc motor with a field winding.

of one stator pole to the next) in the armature-winding conductors, thus producing a dc voltage and a dc current at the terminals of the armature winding. The armature winding, in fact, is a continuous winding, without any beginning or end, and it is connected to the commutator segments. These commutator segments, usually made up of copper, are insulated from each other and rotate with the shaft. At least one pair of stationary carbon brushes is used to make contact between the commutator segments (and, hence, the armature conductors), and the stationary terminals of the armature winding that supply the dc voltage and current.

In a dc motor, the electromagnetic torque is produced by the interaction of the field flux  $\phi_f$  and the armature current  $i_a$ :

$$T_{em} = k_t \phi_f i_a \quad (13-2)$$

where  $k_t$  is the torque constant of the motor. In the armature circuit, a back-emf is produced by the rotation of armature conductors at a speed  $\omega_m$  in the presence of a field flux  $\phi_f$ :

$$e_a = k_e \phi_f \omega_m \quad (13-3)$$

where  $k_e$  is the voltage constant of the motor.

In SI units,  $k_t$  and  $k_e$  are numerically equal, which can be shown by equating the electrical power  $e_a i_a$  and the mechanical power  $\omega_m T_{em}$ . The electrical power is calculated as

$$P_e = e_a i_a = k_e \phi_f \omega_m i_a \quad (\text{using Eq. 13-3}) \quad (13-4)$$

and the mechanical power as

$$P_m = \omega_m T_{em} = k_t \phi_f \omega_m i_a \quad (\text{using Eq. 13-2}) \quad (13-5)$$

In steady state,

$$P_e = P_m \quad (13-6)$$

Therefore, from the foregoing equations

$$k_t \left[ \frac{\text{Nm}}{\text{A} \cdot \text{Wb}} \right] = k_e \left[ \frac{\text{V}}{\text{Wb} \cdot \text{rad/s}} \right] \quad (13-7)$$

In practice, a controllable voltage source  $v_t$  is applied to the armature terminals to establish  $i_a$ . Therefore, the current  $i_a$  in the armature circuit is determined by  $v_t$ , the induced back-emf  $e_a$ , the armature-winding resistance  $R_a$ , and the armature-winding inductance  $L_a$ :

$$v_t = e_a + R_a i_a + L_a \frac{di_a}{dt} \quad (13-8)$$

Equation 13-8 is illustrated by an equivalent circuit in Fig. 13-2.

The interaction of  $T_{em}$  with the load torque, as given by Eq. 12-3b of Chapter 12, determines how the motor speed builds up:

$$T_{em} = J \frac{d\omega_m}{dt} + B\omega_m + T_{WL}(t) \quad (13-9)$$

where  $J$  and  $B$  are the total equivalent inertia and damping, respectively, of the motor-load combination and  $T_{WL}$  is the equivalent working torque of the load.

Seldom are dc machines used as generators. However, they act as generators while braking, where their speed is being reduced. Therefore, it is important to consider dc

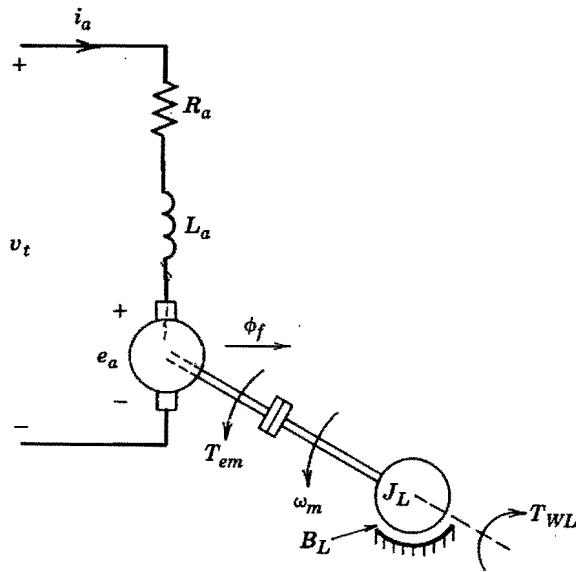


Figure 13-2 A dc motor equivalent circuit.

machines in their generator mode of operation. In order to consider braking, we will assume that the flux  $\phi_f$  is kept constant and the motor is initially driving a load at a speed of  $\omega_m$ . To reduce the motor speed, if  $v_t$  is reduced below  $e_a$  in Fig. 13-2, then the current  $i_a$  will reverse in direction. The electromagnetic torque  $T_{em}$  given by Eq. 13-2 now reverses in direction and the kinetic energy associated with the motor load inertia is converted into electrical energy by the dc machine, which now acts as a generator. This energy must be somehow absorbed by the source of  $v_t$  or dissipated in a resistor.

During the braking operation, the polarity of  $e_a$  does not change, since the direction of rotation has not changed. Equation 13-3 still determines the magnitude of the induced emf. As the rotor slows down,  $e_a$  decreases in magnitude (assuming that  $\phi_f$  is constant). Ultimately, the generation stops when the rotor comes to a standstill and all the inertial energy is extracted. If the terminal-voltage polarity is also reversed, the direction of rotation of the motor will reverse. Therefore, a dc motor can be operated in either direction and its electromagnetic torque can be reversed for braking, as shown by the four quadrants of the torque-speed plane in Fig. 13-3.

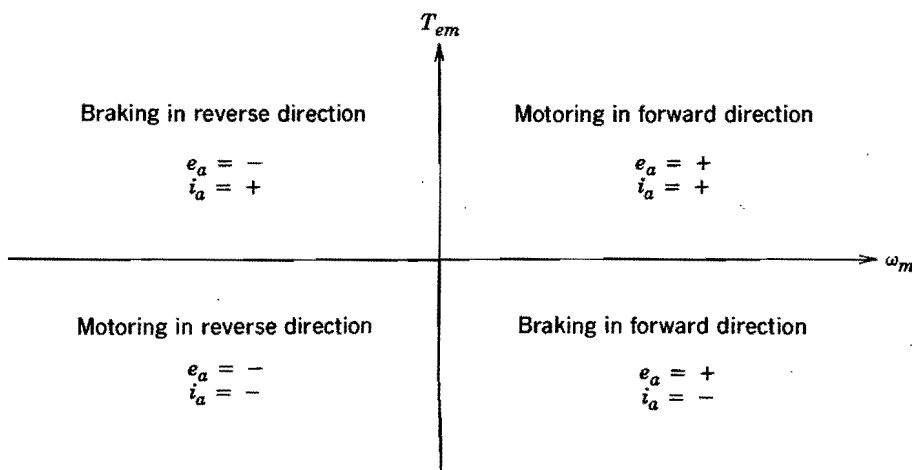


Figure 13-3 Four-quadrant operation of a dc motor.

### 13-3 PERMANENT-MAGNET dc MOTORS

Often in small dc motors, permanent magnets on the stator as shown in Fig. 13-1a produce a constant field flux  $\phi_f$ . In steady state, assuming a constant field flux  $\phi_f$ , Eqs. 13-2, 13-3, and 13-8 result in

$$T_{em} = k_T I_a \quad (13-10)$$

$$E_a = k_E \omega_m \quad (13-11)$$

$$V_t = E_a + R_a I_a \quad (13-12)$$

where  $k_T = k_f \phi_f$  and  $K_E = K_e \phi_f$ . Equations 13-10 through 13-12 correspond to the equivalent circuit of Fig. 13-4a. From the above equations, it is possible to obtain the steady-state speed  $\omega_m$  as a function of  $T_{em}$  for a given  $V_t$ :

$$\omega_m = \frac{1}{k_E} \left( V_t - \frac{R_a}{k_T} T_{em} \right) \quad (13-13)$$

The plot of this equation in Fig. 13-4b shows that as the torque is increased, the torque-speed characteristic at a given  $V_t$  is essentially vertical, except for the droop due to the voltage drop  $I_a R_a$  across the armature-winding resistance. This droop in speed is quite small in integral horsepower dc motors but may be substantial in small servo motors. More importantly, however, the torque-speed characteristics can be shifted horizontally

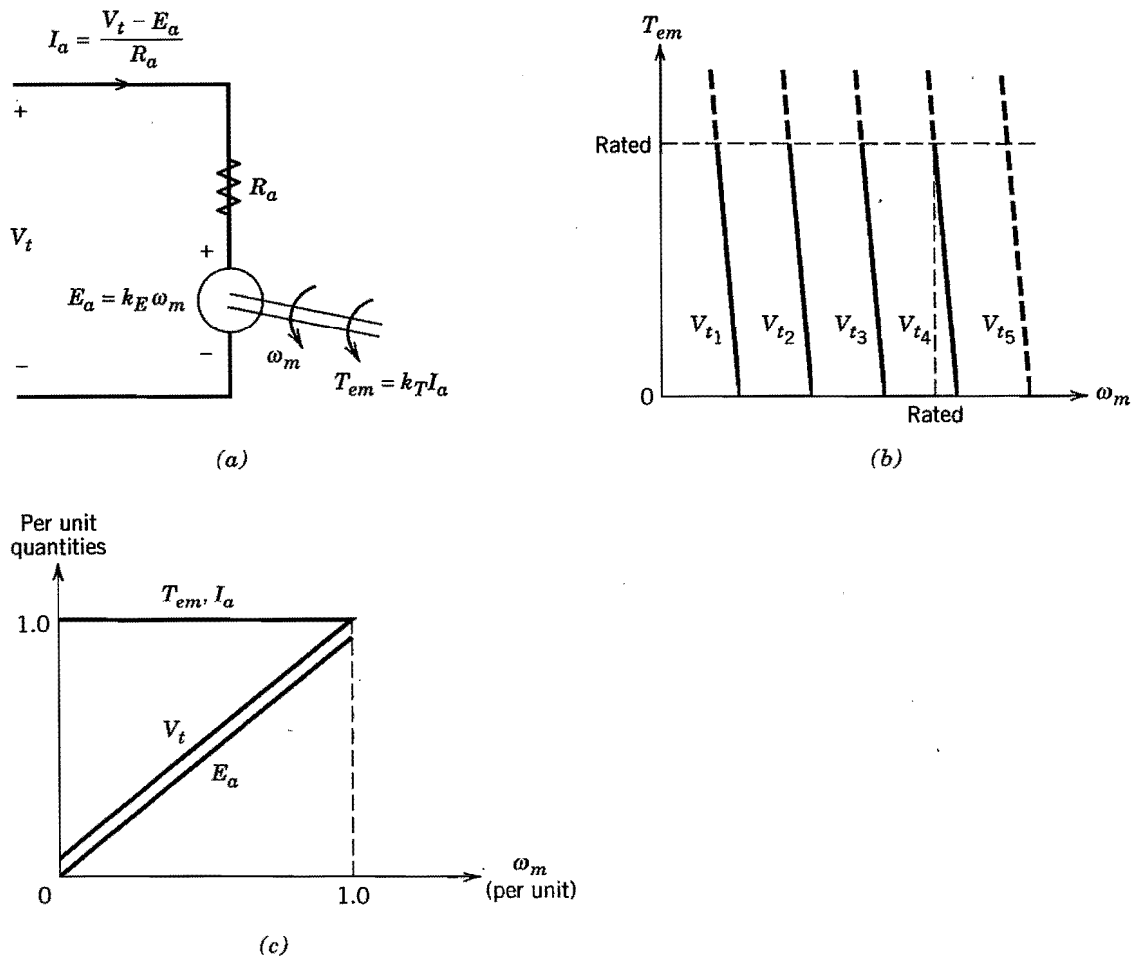


**Figure 13-4** Permanent-magnet dc motor: (a) equivalent circuit; (b) torque-speed characteristics:  $V_{t5} > V_{t4} > V_{t3} > V_{t2} > V_{t1}$ , where  $V_{t4}$  is the rated voltage; (c) continuous torque-speed capability.

in Fig. 13-4*b* by controlling the applied terminal voltage  $V_t$ . Therefore, the speed of a load with an arbitrary torque–speed characteristic can be controlled by controlling  $V_t$  in a permanent-magnet dc motor with a constant  $\phi_f$ .

In a continuous steady state, the armature current  $I_a$  should not exceed its rated value, and therefore, the torque should not exceed the rated torque. Therefore, the characteristics beyond the rated torque are shown as dashed in Fig. 13-4*b*. Similarly, the characteristic beyond the rated speed is shown as dashed, because increasing the speed beyond the rated speed would require the terminal voltage  $V_t$  to exceed its rated value, which is not desirable. This is a limitation of permanent-magnet dc motors, where the maximum speed is limited to the rated speed of the motor. The torque capability as a function of speed is plotted in Fig. 13-4*c*. It shows the steady-state operating limits of the torque and current; it is possible to significantly exceed current and torque limits on a short-term basis. Figure 13-4*c* also shows the terminal voltage required as a function of speed and the corresponding  $E_a$ .

## 13-4 dc MOTORS WITH A SEPARATELY EXCITED FIELD WINDING

Permanent-magnet dc motors are limited to ratings of a few horsepower and also have a maximum speed limitation. These limitations can be overcome if  $\phi_f$  is produced by means of a field winding on the stator, which is supplied by a dc current  $I_f$ , as shown in Fig. 13-1*b*. To offer the most flexibility in controlling the dc motor, the field winding is excited by a separately controlled dc source  $v_f$ , as shown in Fig. 13-5*a*. As indicated by Eq. 13-1, the steady-state value of  $\phi_f$  is controlled by  $I_f (= V_f/R_f)$ , where  $R_f$  is the resistance of the field winding.

Since  $\phi_f$  is controllable, Eq. 13-13 can be written as follows:

$$\omega_m = \frac{1}{k_e \phi_f} \left( V_t - \frac{R_a}{k_t \phi_f} T_{em} \right) \quad (13-14)$$

recognizing that  $k_E = k_e \phi_f$  and  $k_T = k_t \phi_f$ . Equation 13-14 shows that in a dc motor with a separately excited field winding, both  $V_t$  and  $\phi_f$  can be controlled to yield the desired torque and speed. As a general practice, to maximize the motor torque capability,  $\phi_f$  (hence  $I_f$ ) is kept at its rated value for speeds less than the rated speed. With  $\phi_f$  at its rated value, the relationships are the same as given by Eqs. 13-10 through 13-13 of a permanent-magnet dc motor. Therefore, the torque–speed characteristics are also the same as those for a permanent-magnet dc motor that were shown in Fig. 13-4*b*. With  $\phi_f$  constant and equal to its rated value, the motor torque–speed capability is as shown in Fig. 13-5*b*, where this region of constant  $\phi_f$  is often called the constant-torque region. The required terminal voltage  $V_t$  in this region increases linearly from approximately zero to its rated value as the speed increases from zero to its rated value. The voltage  $V_t$  and the corresponding  $E_a$  are shown in Fig. 13-5*b*.

To obtain speeds beyond its rated value,  $V_t$  is kept constant at its rated value and  $\phi_f$  is decreased by decreasing  $I_f$ . Since  $I_a$  is not allowed to exceed its rated value on a continuous basis, the torque capability declines, since  $\phi_f$  is reduced in Eq. 13-2. In this so-called field-weakening region, the maximum power  $E_a I_a$  (equal to  $\omega_m T_{em}$ ) into the motor is not allowed to exceed its rated value on a continuous basis. This region, also called the constant-power region, is shown in Fig. 13-5*b*, where  $T_{em}$  declines with  $\omega_m$  and  $V_t$ ,  $E_a$ , and  $I_a$  stay constant at their rated values. It should be emphasized that Fig. 13-5*b* is the plot of the maximum continuous capability of the motor in steady state. Any

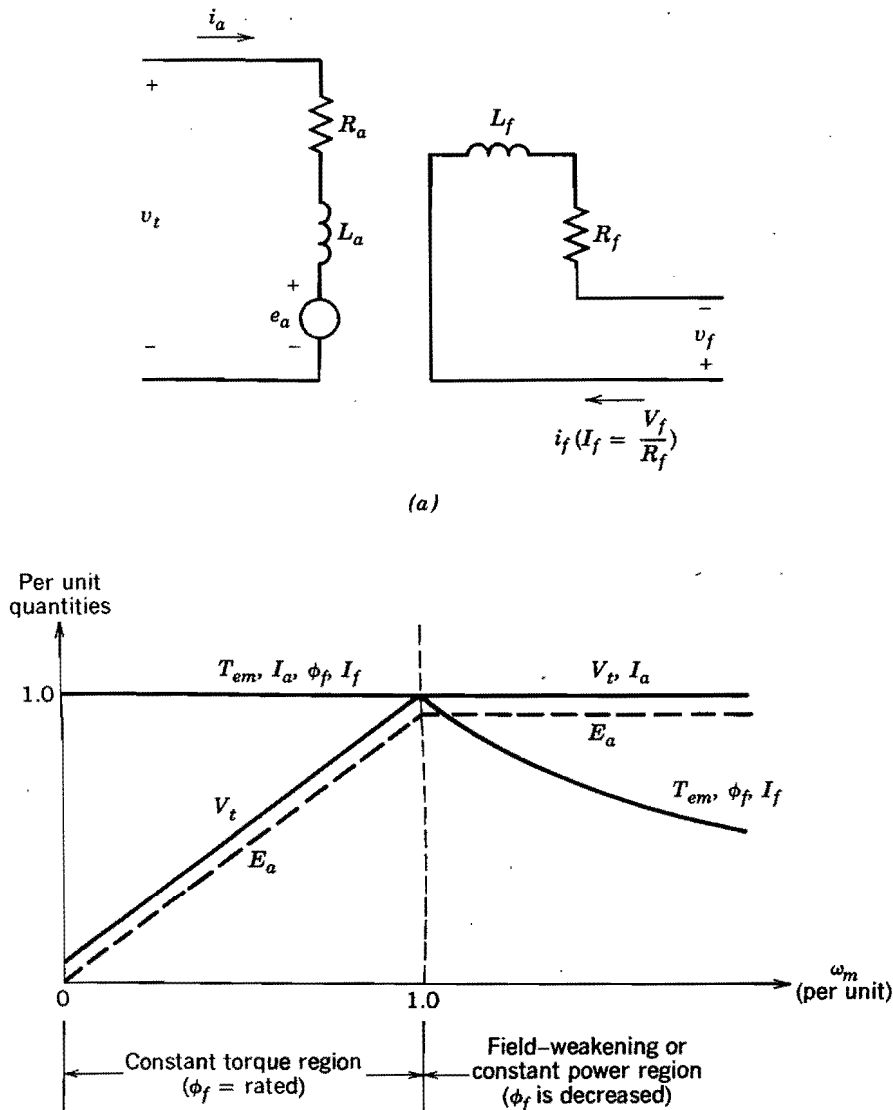


**Figure 13-5** Separately excited dc motor: (a) equivalent circuit; (b) continuous torque-speed capability.

operating point within the regions shown is, of course, permissible. In the field-weakening region, the speed may be exceeded by 50–100% of its rated value, depending on the motor specifications.

## 13-5 EFFECT OF ARMATURE CURRENT WAVEFORM

In dc motor drives, the output voltage of the power electronic converter contains an ac ripple voltage superimposed on the desired dc voltage. Ripple in the terminal voltage can lead to a ripple in the armature current with the following consequences that must be recognized: the form factor and torque pulsations.

### 13-5-1 FORM FACTOR

The form factor for the dc motor armature current is defined as

$$\text{Form factor} = \frac{I_a(\text{rms})}{I_a(\text{average})} \quad (13-15)$$



The form factor will be unity only if  $i_a$  is a pure dc. The more  $i_a$  deviates from a pure dc, the higher will be the value of the form factor. The power input to the motor (and hence the power output) varies proportionally with the average value of  $i_a$ , whereas the losses in the resistance of the armature winding depend on  $I_a^2(\text{rms})$ . Therefore, the higher the form factor of the armature current, the higher the losses in the motor (i.e., higher heating) and, hence, the lower the motor efficiency.

Moreover, a form factor much higher than unity implies a much larger value of the peak armature current compared to its average value, which may result in excessive arcing in the commutator and brushes. To avoid serious damage to the motor that is caused by large peak currents, the motor may have to be derated (i.e., the maximum power or torque would have to be kept well below its rating) to keep the motor temperature from exceeding its specified limit and to protect the commutator and brushes. Therefore, it is desirable to improve the form factor of the armature current as much as possible.

### 13-5-2 TORQUE PULSATIONS

Since the instantaneous electromagnetic torque  $T_{em}(t)$  developed by the motor is proportional to the instantaneous armature current  $i_a(t)$ , a ripple in  $i_a$  results in a ripple in the torque and hence in speed if the inertia is not large. This is another reason to minimize the ripple in the armature current. It should be noted that a high-frequency torque ripple will result in smaller speed fluctuations, as compared with a low-frequency torque ripple of the same magnitude.

## 13-6 dc SERVO DRIVES

In servo applications, the speed and accuracy of response is important. In spite of the increasing popularity of ac servo drives, dc servo drives are still widely used. If it were not for the disadvantages of having a commutator and brushes, the dc motors would be ideally suited for servo drives. The reason is that the instantaneous torque  $T_{em}$  in Eq. 13-2 can be controlled linearly by controlling the armature current  $i_a$  of the motor.

### 13-6-1 TRANSFER FUNCTION MODEL FOR SMALL-SIGNAL DYNAMIC PERFORMANCE

Figure 13-6 shows a dc motor operating in a closed loop to deliver controlled speed or controlled position. To design the proper controller that will result in high performance (high speed of response, low steady-state error, and high degree of stability), it is im-

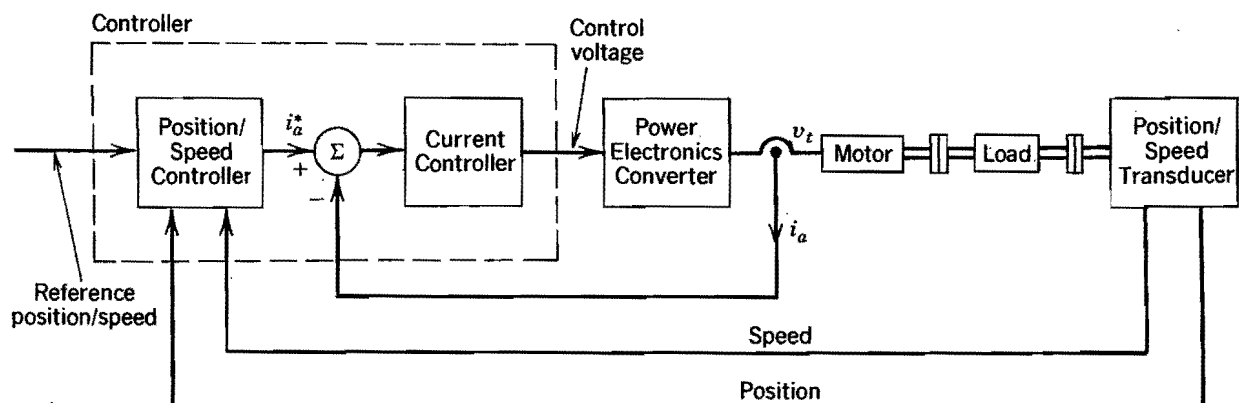


Figure 13-6 Closed-loop position/speed dc servo drive.

portant to know the transfer function of the motor. It is then combined with the transfer function of the rest of the system in order to determine the dynamic response of the drive for changes in the desired speed and position or for a change in load. As we will explain later on, the linear model is valid only for small changes where the motor current is not limited by the converter supplying the motor.

For analyzing small-signal dynamic performance of the motor-load combination around a steady-state operating point, the following equations can be written in terms of small deviations around their steady-state values:

$$\Delta v_t = \Delta e_a + R_a \Delta i_a + L_a \frac{d}{dt} (\Delta i_a) \quad (13-16)$$

$$\Delta e_a = k_E \Delta \omega_m \quad (13-17)$$

$$\Delta T_{em} = k_T \Delta i_a \quad (13-18)$$

$$\Delta T_{em} = \Delta T_{WL} + B \Delta \omega_m + J \frac{d(\Delta \omega_m)}{dt} \quad (\text{from Eq. 13-9}) \quad (13-19)$$

If we take the Laplace transform of these equations, where the Laplace variables represent only the small-signal  $\Delta$  values in Eqs. 13-16 through 13-19,

$$V_t(s) = E_a(s) + (R_a + sL_a)I_a(s)$$

$$E_a(s) = k_E \omega_m(s)$$

$$T_{em}(s) = k_T I_a(s)$$

$$T_{em}(s) = T_{WL}(s) + (B + sJ)\omega_m(s)$$

$$\omega_m(s) = s\theta_m(s)$$

(13-20)

These equations for the motor-load combination can be represented by transfer function blocks, as shown in Fig. 13-7. The inputs to the motor-load combination in Fig. 13-7 are the armature terminal voltage  $V_t(s)$  and the load torque  $T_{WL}(s)$ . Applying one input at a time by setting the other input to zero, the superposition principle yields (note that this is a linearized system)

$$\omega_m(s) = \frac{k_T}{(R_a + sL_a)(sJ + B) + k_T k_E} V_t(s) - \frac{R_a + sL_a}{(R_a + sL_a)(sJ + B) + k_T k_E} T_{WL}(s) \quad (13-21)$$

This equation results in two closed-loop transfer functions:

$$G_1(s) = \left. \frac{\omega_m(s)}{V_t(s)} \right|_{T_{WL}(s)=0} = \frac{k_T}{(R_a + sL_a)(sJ + B) + k_T k_E} \quad (13-22)$$

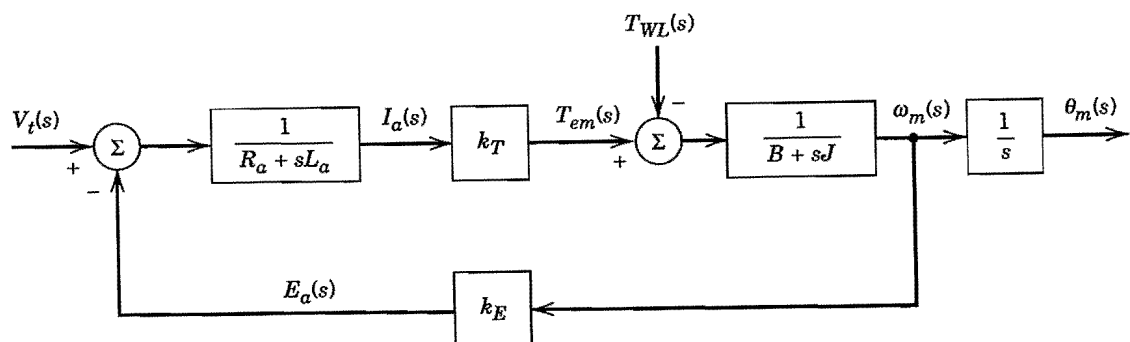


Figure 13-7 Block diagram representation of the motor and load (without any feedback).

$$G_2(s) = \left. \frac{\omega_m(s)}{T_{WL}(s)} \right|_{V_t(s)=0} = -\frac{R_a + sL_a}{(R_a + sL_a)(sJ + B) + k_T k_E} \quad (13-23)$$

As a simplification to gain better insight into the dc motor behavior, the friction term, which is usually small, will be neglected by setting  $B = 0$  in Eq. 13-22. Moreover, considering just the motor without the load,  $J$  in Eq. 13-22 is then the motor inertia  $J_m$ . Therefore

$$G_1(s) = \frac{k_T}{sJ_m(R_a + sL_a) + k_T k_E} = \frac{1}{k_E \left( s^2 \frac{L_a J_m}{k_T k_E} + s \frac{R_a J_m}{k_T k_E} + 1 \right)} \quad (13-24)$$

We will define the following constants:

$$\tau_m = \frac{R_a J_m}{k_T k_E} = \text{mechanical time constant} \quad (13-25)$$

$$\tau_e = \frac{L_a}{R_a} = \text{electrical time constant} \quad (13-26)$$

Using  $\tau_m$  and  $\tau_e$  in the expression for  $G_1(s)$  yields

$$G_1(s) = \frac{1}{k_E(s^2 \tau_m \tau_e + s\tau_m + 1)} \quad (13-27)$$

Since in general  $\tau_m \gg \tau_e$ , it is a reasonable approximation to replace  $s\tau_m$  by  $s(\tau_m + \tau_e)$  in the foregoing expression. Therefore

$$G_1(s) = \frac{\omega_m(s)}{V_t(s)} \approx \frac{1}{k_E(s\tau_m + 1)(s\tau_e + 1)} \quad (13-28)$$

The physical significance of the electrical and the mechanical time constants of the motor should also be understood. The electrical time constant  $\tau_e$  determines how quickly the armature current builds up, as shown in Fig. 13-8, in response to a step change  $\Delta v_t$  in the terminal voltage, where the rotor speed is assumed to be constant.

The mechanical time constant  $\tau_m$  determines how quickly the speed builds up in response to a step change  $\Delta v_t$  in the terminal voltage, provided that the electrical time constant  $\tau_e$  is assumed to be negligible and, hence, the armature current can change

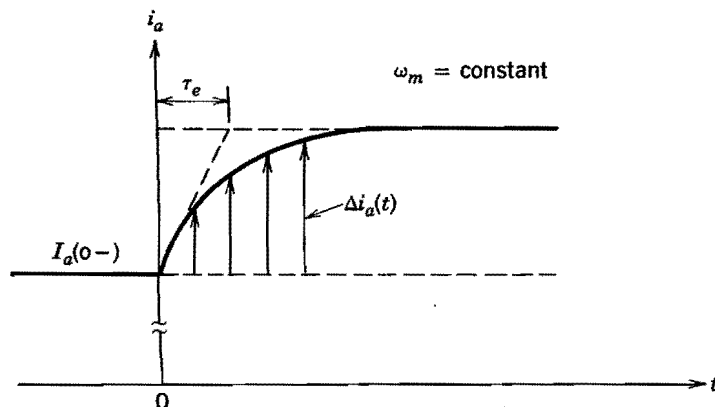


**Figure 13-8** Electrical time constant  $\tau_e$ ; speed  $\omega_m$  is assumed to be constant.

instantaneously. Neglecting  $\tau_e$  in Eq. 13-28, the change in speed from the steady-state condition can be obtained as

$$\omega_m(s) = \frac{V_t(s)}{k_E(s\tau_m + 1)} = \frac{\Delta v_t}{k_E s(s\tau_m + 1)} = \frac{\Delta v_t}{k_E} \frac{1/\tau_m}{s(s + 1/\tau_m)} \quad (13-29)$$

recognizing that  $V_t(s) = \Delta v_t/s$ . From Eq. 13-29

$$\Delta\omega_m(t) = \frac{\Delta v_t}{k_E} (1 - e^{-t/\tau_m}) \quad (13-30)$$

where  $\tau_m$  is the mechanical time constant with which the speed changes in response to a step change in the terminal voltage, as shown in Fig. 13-9a. The corresponding change in the armature current is plotted in Fig. 13-9b. Note that if the motor current is limited by the converter during large transients, the torque produced by the motor is simply  $k_T I_{a,\max}$ .

### 13-6-2 POWER ELECTRONIC CONVERTER

Based on the previous discussion, a power electronic converter supplying a dc motor should have the following capabilities:

1. The converter should allow both its output voltage and current to reverse in order to yield a four-quadrant operation as shown in Fig. 13-3.
2. The converter should be able to operate in a current-controlled mode by holding the current at its maximum acceptable value during fast acceleration and deceleration. The dynamic current limit is generally several times higher than the continuous steady-state current rating of the motor.
3. For accurate control of position, the average voltage output of the converter should vary linearly with its control input, independent of the load on the motor. This item is further discussed in Section 13-6-5.
4. The converter should produce an armature current with a good form factor and should minimize the fluctuations in torque and speed of the motor.

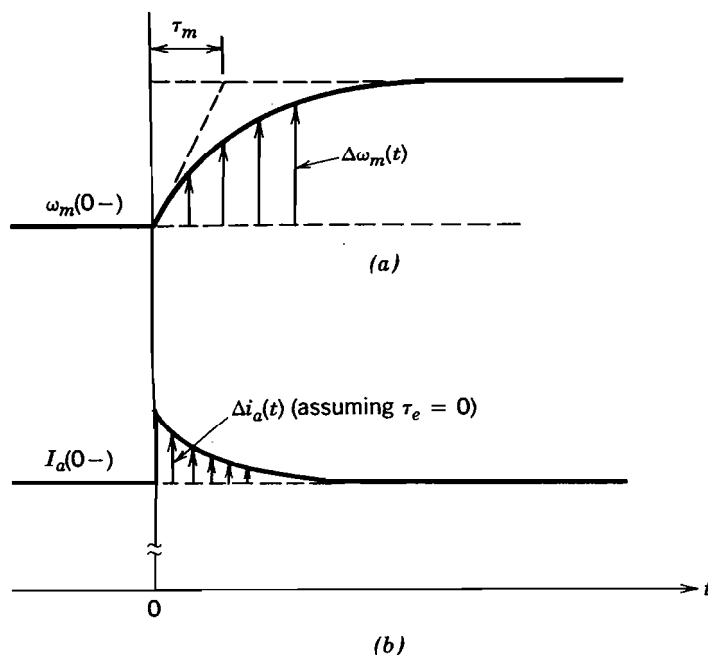


**Figure 13-9**  
Mechanical time constant  $\tau_m$ ; load torque is assumed to be constant.

5. The converter output should respond as quickly as possible to its control input, thus allowing the converter to be represented essentially by a constant gain without a dead time in the overall servo drive transfer function model.

A linear power amplifier satisfies all the requirements listed above. However, because of its low energy efficiency, this choice is limited to a very low power range. Therefore, the choice must be made between switch-mode dc-dc converters of the type discussed in Chapter 7 or the line-frequency-controlled converters discussed in Chapter 6. Here, only the switch-mode dc-dc converters are described. Drives with line-frequency converters can be analyzed in the same manner.

A full-bridge switch-mode dc-dc converter produces a four-quadrant controllable dc output. This full-bridge dc-dc converter (also called an H-bridge) was discussed in Chapter 7. The overall system is shown in Fig. 13-10, where the line-frequency ac input is rectified into dc by means of a diode rectifier of the type discussed in Chapter 5 and filtered by means of a filter capacitor. An energy dissipation circuit is included to prevent the filter capacitor voltage from becoming large in case of braking of the dc motor.

As discussed in Chapter 7, all four switches in the converter of Fig. 13-10 are switched during each cycle of the switching frequency. This results in a true four-quadrant operation with a continuous-current conduction, where both  $V_t$  and  $I_a$  can smoothly reverse, independent of each other. Ignoring the effect of blanking time, the average voltage output of the converter varies linearly with the input control voltage  $v_{\text{control}}$ , independent of the load:

$$V_t = k_c v_{\text{control}} \quad (13-31)$$

where  $k_c$  is the gain of the converter.

As discussed in Sections 7-7-1 and 7-7-2 of Chapter 7, either a PWM bipolar voltage-switching scheme or a PWM unipolar voltage-switching scheme can be used. Thus, the converter in Fig. 13-6 can be replaced by an amplifier gain  $k_c$  given by Eq. 13-31.

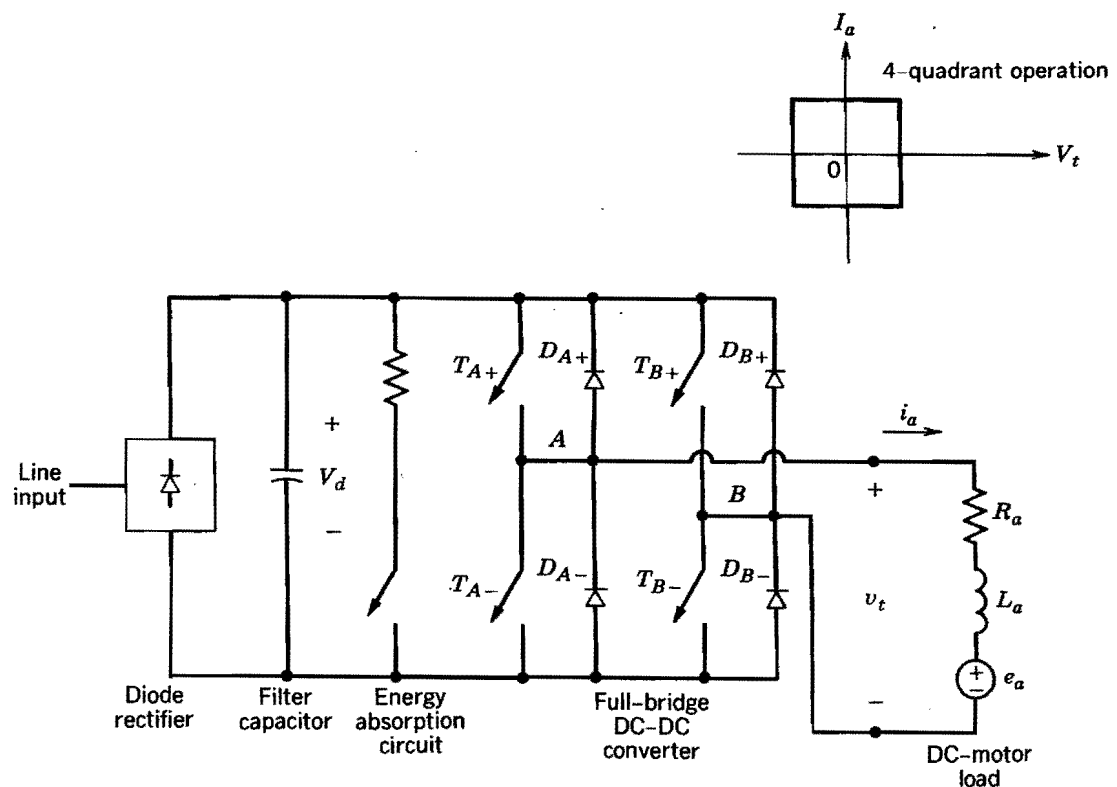


Figure 13-10 A dc motor servo drive; four-quadrant operation.

### 13-6-3 RIPPLE IN THE ARMATURE CURRENT $i_a$

In Chapter 7, it was mentioned that the current through a PWM full-bridge dc-dc converter supplying a dc motor load flows continuously even at small values of  $I_a$ . However, it is important to consider the peak-to-peak ripple in the armature current because of its impact on the torque pulsations and heating of the motor. Moreover, a larger current ripple requires a larger peak current rating of the converter switches.

In the system of Fig. 13-10 under a steady-state operating condition, the instantaneous speed  $\omega_m$  can be assumed to be constant if there is sufficient inertia, and therefore  $e_a(t) = E_a$ . The terminal voltage and the armature current can be expressed in terms of their dc and the ripple components as

$$v_t(t) = V_t + v_r(t) \quad (13-32)$$

$$i_a(t) = I_a + i_r(t) \quad (13-33)$$

where  $v_r(t)$  and  $i_r(t)$  are the ripple components in  $v_t$  and  $i_a$ , respectively. Therefore, in the armature circuit, from Eq. 13-8,

$$V_t + v_r(t) = E_a + R_a[I_a + i_r(t)] + L_a \frac{di_r(t)}{dt} \quad (13-34)$$

where

$$V_t = E_a + R_a I_a \quad (13-35)$$

and

$$v_r(t) = R_a i_r(t) + L_a \frac{di_r(t)}{dt} \quad (13-36)$$

Assuming that the ripple current is primarily determined by the armature inductance  $L_a$  and  $R_a$  has a negligible effect, from Eq. 13-36

$$v_r(t) \approx L_a \frac{di_r(t)}{dt} \quad (13-37)$$

The additional heating in the motor is approximately  $R_a I_r^2$ , where  $I_r$  is the rms value of the ripple current  $i_r$ .

By means of an example and Fig. 7-30, it was shown in Chapter 7 that for a PWM bipolar voltage switching, the ripple voltage is maximum when the average output voltage is zero and all switches operate at equal duty ratios. Applying these results to the dc motor drive, Fig. 13-11a shows the voltage ripple  $v_r(t)$  and the resulting ripple current  $i_r(t)$  using Eq. 13-37. From these waveforms, the maximum peak-to-peak ripple can be calculated as

$$(\Delta I_{p-p})_{\max} = \frac{V_d}{2L_a f_s} \quad (13-38)$$

where  $V_d$  is the input dc voltage to the full-bridge converter.

The ripple voltage for a PWM unipolar voltage switching is shown to be maximum when the average output voltage is  $\frac{1}{2} V_d$ . Applying this result to a dc motor drive, Fig. 13-11b shows  $i_r(t)$  waveform, where

$$(\Delta I_{p-p})_{\max} = \frac{V_d}{8L_a f_s} \quad (13-39)$$

Equations 13-38 and 13-39 show that the maximum peak-to-peak ripple current is inversely proportional to  $L_a$  and  $f_s$ . Therefore, careful consideration must be given to the

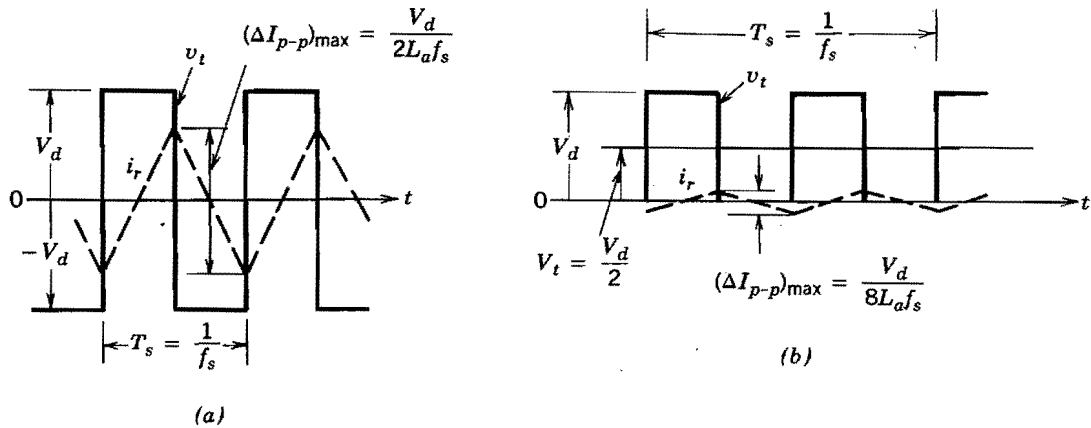


**Figure 13-11** Ripple  $i_r$  in the armature current: (a) PWM bipolar voltage switching,  $V_t = 0$ ; (b) PWM unipolar voltage switching,  $V_t = \frac{1}{2}V_d$ .

selection of  $f_s$  and  $L_a$ , where  $L_a$  can be increased by adding an external inductor in the series with the motor armature.

#### 13-6-4 CONTROL OF SERVO DRIVES

A servo system where the speed error directly controls the power electronic converter is shown in Fig. 13-12a. The current-limiting circuit comes into operation only when the drive current tries to exceed an acceptable limit  $I_{a,\max}$  during fast accelerations and decelerations. During these intervals, the output of the speed regulator is suppressed and the current is held at its limit until the speed and position approach their desired values.

To improve the dynamic response in high-performance servo drives, an internal current loop is used as shown in Fig. 13-12b, where the armature current and, hence, the torque are controlled. The current control is accomplished by comparing the actual measured armature current  $i_a$  with its reference value  $i_a^*$  produced by the speed regulator. The current  $i_a$  is inherently controlled from exceeding the current rating of the drive by limiting the reference current  $i_a^*$  to  $I_{a,\max}$ .

The armature current provided by the dc-dc converter in Fig. 13-12b can be controlled in a similar manner as the current-regulated modulation in a dc-to-ac inverter, discussed in Section 8-6-3. The only difference is that the reference current in steady state in a dc-dc converter is a dc rather than a sinusoidal waveform as in Section 8-6-3. Either a variable-frequency tolerance band control, discussed in Section 8-6-3-1, or a fixed-frequency control, discussed in Section 8-6-3-2, can be used for current control.

#### 13-6-5 NONLINEARITY DUE TO BLANKING TIME

In a practical full-bridge dc-dc converter, where the possibility of a short circuit across the input dc bus exists, a blanking time is introduced between the instant at which a switch turns off and the instant at which the other switch in the same leg turns on. The effect of the blanking time on the output of dc-to-ac full bridge PWM inverters was discussed in detail in Section 8-5. That analysis is also valid for PWM full-bridge dc-dc converters for dc servo drives. Equation 8-77 and Fig. 8-32b show the effect of blanking time on the output voltage magnitude. Recognizing that the output voltage of the converter is proportional to the motor speed  $\omega_m$  and the output current  $i_a$  is proportional to the torque  $T_{em}$ , Fig. 8-32b is redrawn as in Fig. 13-13. If at an arbitrary speed  $\omega_m$ , the torque and, hence,  $i_a$  are to be reversed, there is a dead zone in  $v_{\text{control}}$ , as shown in Fig. 13-13, during which

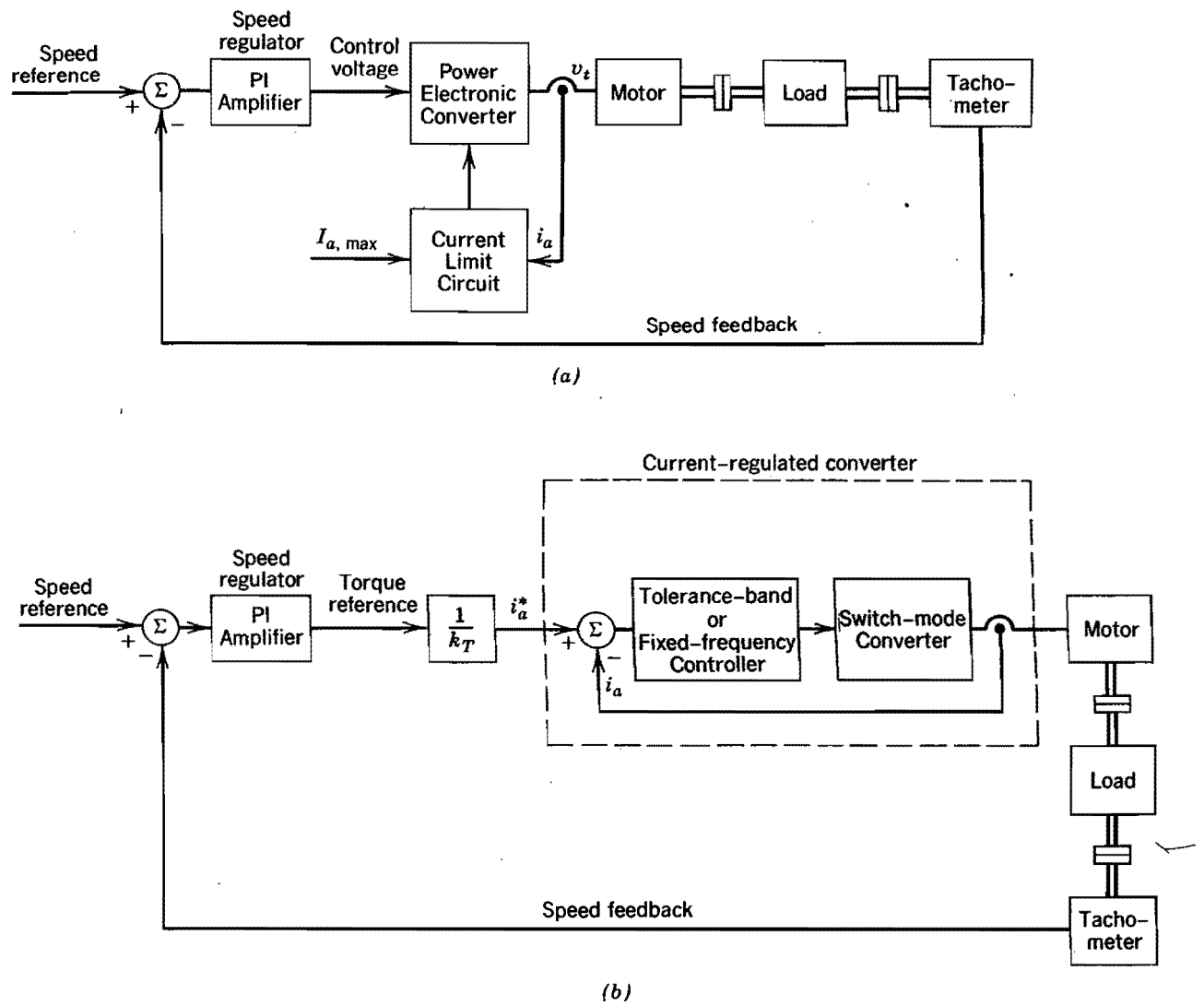


**Figure 13-12** Control of servo drives: (a) no internal current-control loop; (b) internal current-control loop.

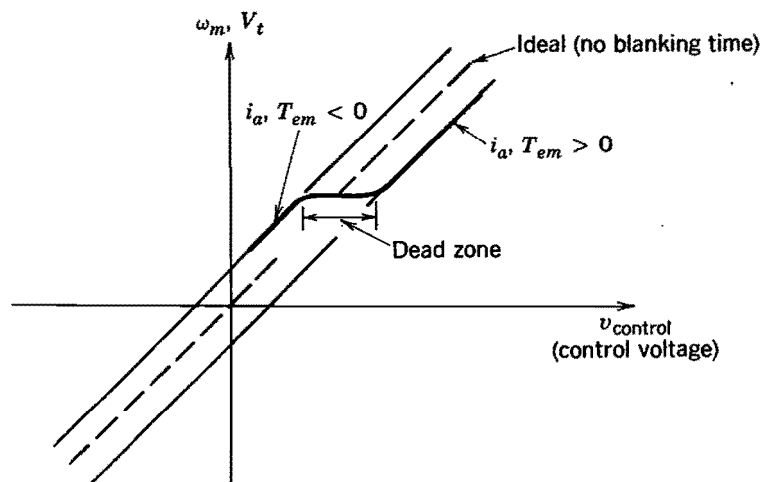


**Figure 13-13** Effect of blanking time.



$i_a$  and  $T_{em}$  remain small. The effect of this nonlinearity due to blanking time on the performance of the servo system is minimized by means of the current-controlled mode of operation discussed in the block diagram of Fig. 13-12b, where an internal current loop directly controls  $i_a$ .

### 13-6-6 SELECTION OF SERVO DRIVE PARAMETERS

Based on the foregoing discussion, the effects of armature inductance  $L_a$ , switching frequency  $f_s$ , blanking time  $t_\Delta$ , and switching times  $t_c$  of the solid state devices in the dc-dc converter can be summarized as follows:

1. The ripple in the armature current, which causes torque ripple and additional armature heating, is proportional to  $L_a/f_s$ .
2. The dead zone in the transfer function of the converter, which degrades the servo performance, is proportional to  $f_s t_\Delta$ .
3. Switching losses in the converter are proportional to  $f_s t_c$ .

All these factors need to be considered simultaneously in the selection of the appropriate motor and the power electronic converter.

## 13-7 ADJUSTABLE-SPEED dc DRIVES

Unlike servo drives, the response time to speed and torque commands is not as critical in adjustable-speed drives. Therefore, either switch-mode dc-dc converters as discussed for servo drives or the line-frequency controlled converters discussed in Chapter 6 can be used for speed control.

### 13-7-1 SWITCH-MODE dc-dc CONVERTER

If a four-quadrant operation is needed and a switch-mode converter is utilized, then the full-bridge converter shown in Fig. 13-10 is used.

If the speed does not have to reverse but braking is needed, then the two-quadrant converter shown in Fig. 13-14a can be used. It consists of two switches, where one of the switches is on at any time, to keep the output voltage independent of the direction of  $i_a$ . The armature current can reverse, and a negative value of  $I_a$  corresponds to the braking mode of operation, where the power flows from the dc motor to  $V_d$ . The output voltage  $V_t$  can be controlled in magnitude, but it always remains unipolar. Since  $i_a$  can flow in both directions, unlike in the single-switch step-down and step-up dc-dc converters discussed in Chapter 7,  $i_a$  in the circuit of Fig. 13-14a will not become discontinuous.

For a single-quadrant operation where the speed remains unidirectional and braking is not required, the step-down converter shown in Fig. 13-14b can be used.

### 13-7-2 LINE-FREQUENCY CONTROLLED CONVERTERS

In many adjustable-speed dc drives, especially in large power ratings, it may be economical to utilize a line-frequency controlled converter of the type discussed in Chapter 6. Two of these converters are repeated in Fig. 13-15 for single-phase and three-phase ac inputs. The output of these line-frequency converters, also called the phase-controlled converters, contains an ac ripple that is a multiple of the 60-Hz line frequency. Because of this low frequency ripple, an inductance in series with the motor armature may be

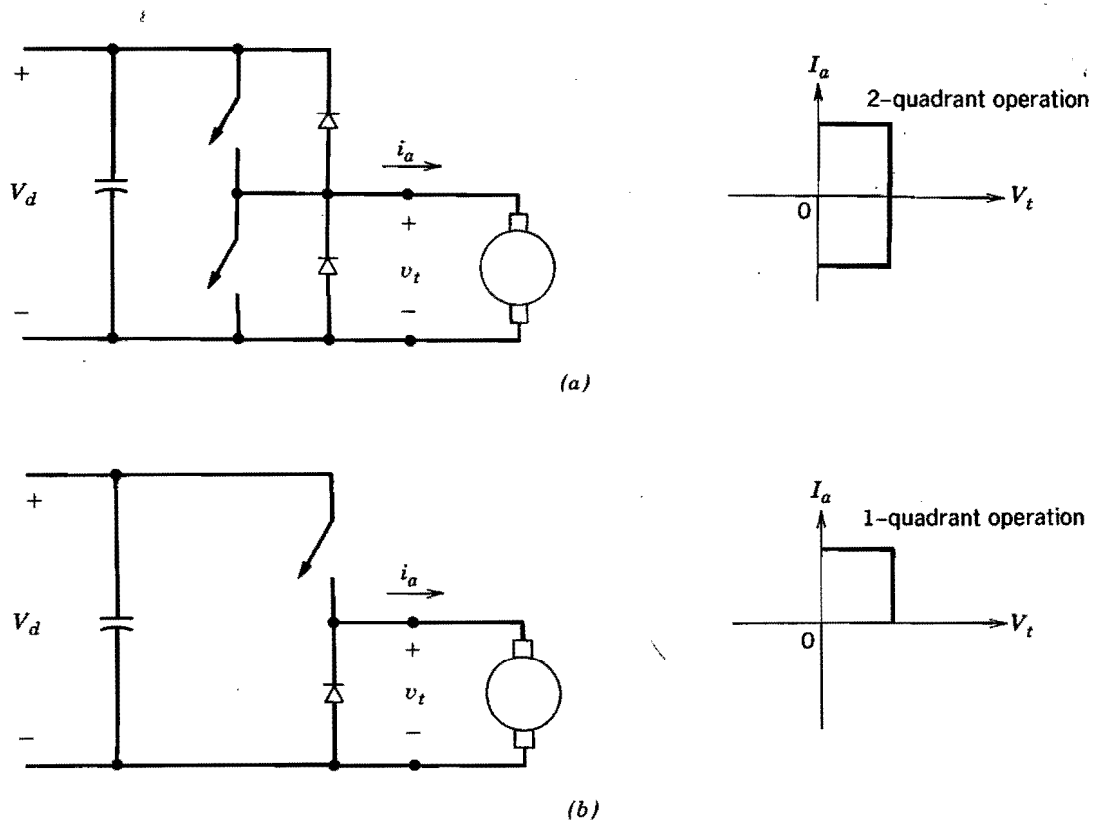


Figure 13-14 (a) Two-quadrant operation; (b) single-quadrant operation.

required to keep the ripple in  $i_a$  low, to minimize its effect on armature heating and the ripple in torque and speed.

A disadvantage of the line-frequency converters is the longer dead time in responding to the changes in the speed control signal, compared to high-frequency switch-mode dc-dc converters. Once a thyristor or a pair of thyristors is triggered on in the circuits of Fig. 13-15, the delay angle  $\alpha$  that controls the converter output voltage applied to the motor terminals cannot be increased for a portion of the 60-Hz cycle. This may not be a problem in adjustable-speed drives where the response time to speed and torque commands is not too critical. But it clearly shows the limitation of line-frequency converters in servo drive applications.

The current through these line-frequency controlled converters is unidirectional, but the output voltage can reverse polarity. The two-quadrant operation with the reversible voltage is not suited for dc motor braking, which requires the voltage to be unidirectional

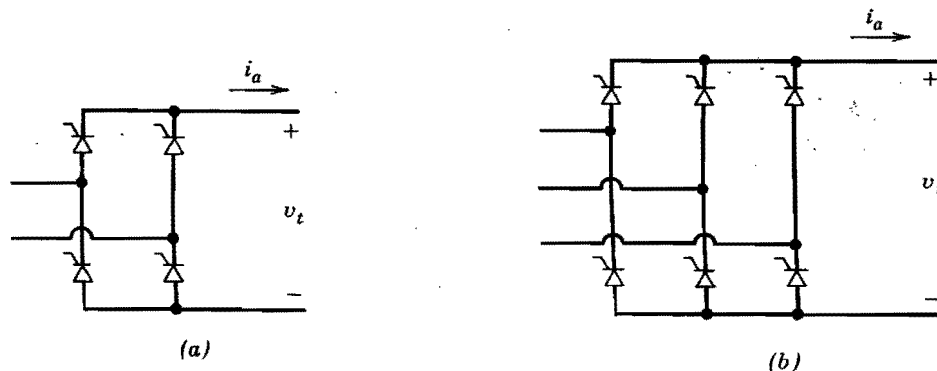
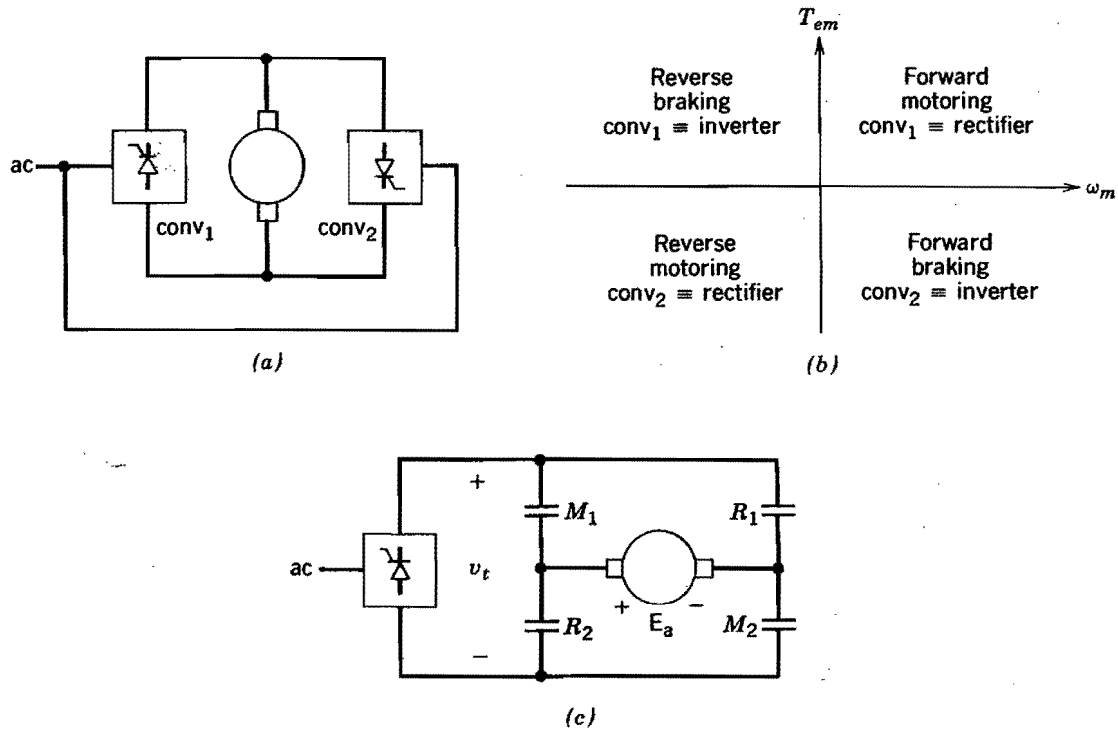


Figure 13-15 Line-frequency-controlled converters for dc motor drives: (a) single-phase input; (b) three-phase input.



**Figure 13-16** Line-frequency-controlled converters for four-quadrant operation: (a) back-to-back converters for four-quadrant operation (without circulating current); (b) converter operation modes; (c) contactors for four-quadrant operation.

but the current to be reversible. Therefore, if regenerative braking is required, two back-to-back connected thyristor converters can be used, as shown in Fig. 13-16a. This, in fact, gives a capability to operate in all four quadrants, as depicted in Fig. 13-16b.

An alternative to using two converters is to use one phase-controlled converter together with two pairs of contactors, as shown in Fig. 13-16c. When the machine is to be operated as a motor, the contactors  $M_1$  and  $M_2$  are closed. During braking when the motor speed is to be reduced rapidly, since the direction of rotation remains the same,  $E_a$  is of the same polarity as in the motoring mode. Therefore, to let the converter go into an inverter mode, contactors  $M_1$  and  $M_2$  are opened and  $R_1$  and  $R_2$  are closed. It should be noted that the contactors switch at zero current when the current through them is brought to zero by the converter.

### 13-7-3 EFFECT OF DISCONTINUOUS ARMATURE CURRENT

In line-frequency phase-controlled converters and single-quadrant step-down switch-mode dc-dc converters, the output current can become discontinuous at light loads on the motor. For a fixed control voltage  $v_{\text{control}}$  or the delay angle  $\alpha$ , the discontinuous current causes the output voltage to go up. This voltage rise causes the motor speed to increase at low values of  $I_a$  (which correspond to low torque load), as shown generically by Fig. 13-17. With a continuously flowing  $i_a$ , the drop in speed at higher torques is due to the voltage drop  $R_a I_a$  across the armature resistance; additional drop in speed occurs in the phase-controlled converter-driven motors due to commutation voltage drops across the ac-side inductance  $L_s$ , which approximately equal  $(2\omega L_s/\pi)I_a$  in single-phase converters and  $(3\omega L_s/\pi)I_a$  in three-phase converters, as discussed in Chapter 6. These effects result in poor speed regulation under an open-loop operation.

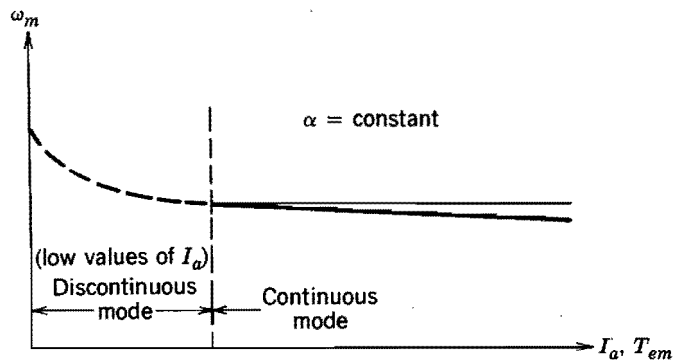


Figure 13-17 Effect of discontinuous  $i_a$  on  $\omega_m$ .

#### 13-7-4 CONTROL OF ADJUSTABLE-SPEED DRIVES

The type of control used depends on the drive requirements. An open-loop control is shown in Fig. 13-18 where the speed command  $\omega^*$  is generated by comparing the drive output with its desired value (which, e.g., may be temperature in case of a capacity-modulated heat pump). A  $d/dt$  limiter allows the speed command to change slowly, thus preventing the rotor current from exceeding its rating. The slope of the  $d/dt$  limiter can be adjusted to match the motor-load inertia. The current limiter in such drives may be just a protective measure, whereby if the measured current exceeds its rated value, the controller shuts the drive off. A manual restart may be required. As discussed in Section 13-6, a closed-loop control can also be implemented.

#### 13-7-5 FIELD WEAKENING IN ADJUSTABLE-SPEED dc MOTOR DRIVES

In a dc motor with a separately excited field winding, the drive can be operated at higher than the rated speed of the motor by reducing the field flux  $\phi_f$ . Since many adjustable-speed drives, especially at higher power ratings, employ a motor with a wound field, this capability can be exploited by controlling the field current and  $\phi_f$ . The simple line-frequency phase-controlled converter shown in Fig. 13-15 is normally used to control  $I_f$  through the field winding, where the current is controlled in magnitude but always flows in only one direction. If a converter topology consisting of only thyristors (such as in Fig. 13-15) is chosen, where the converter output voltage is reversible, the field current can be decreased rapidly.

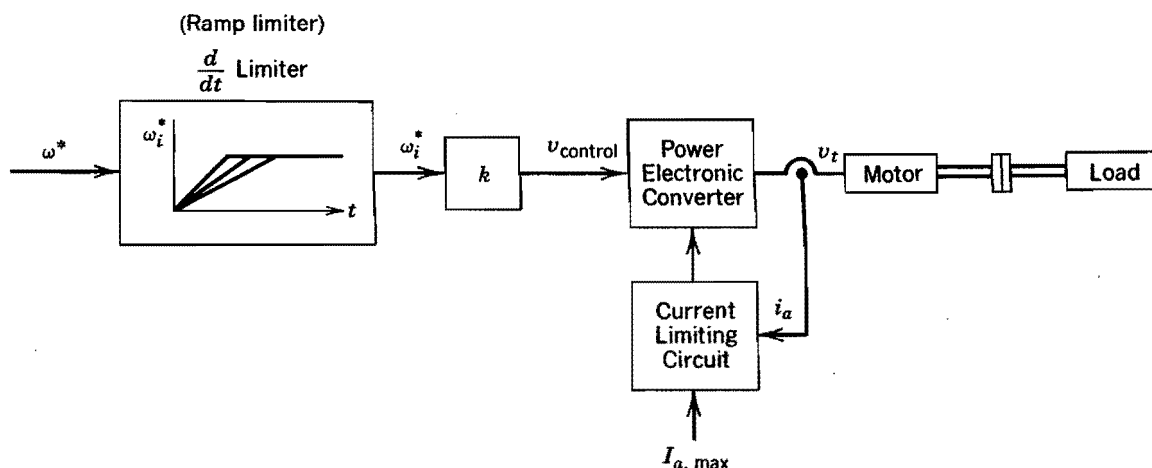
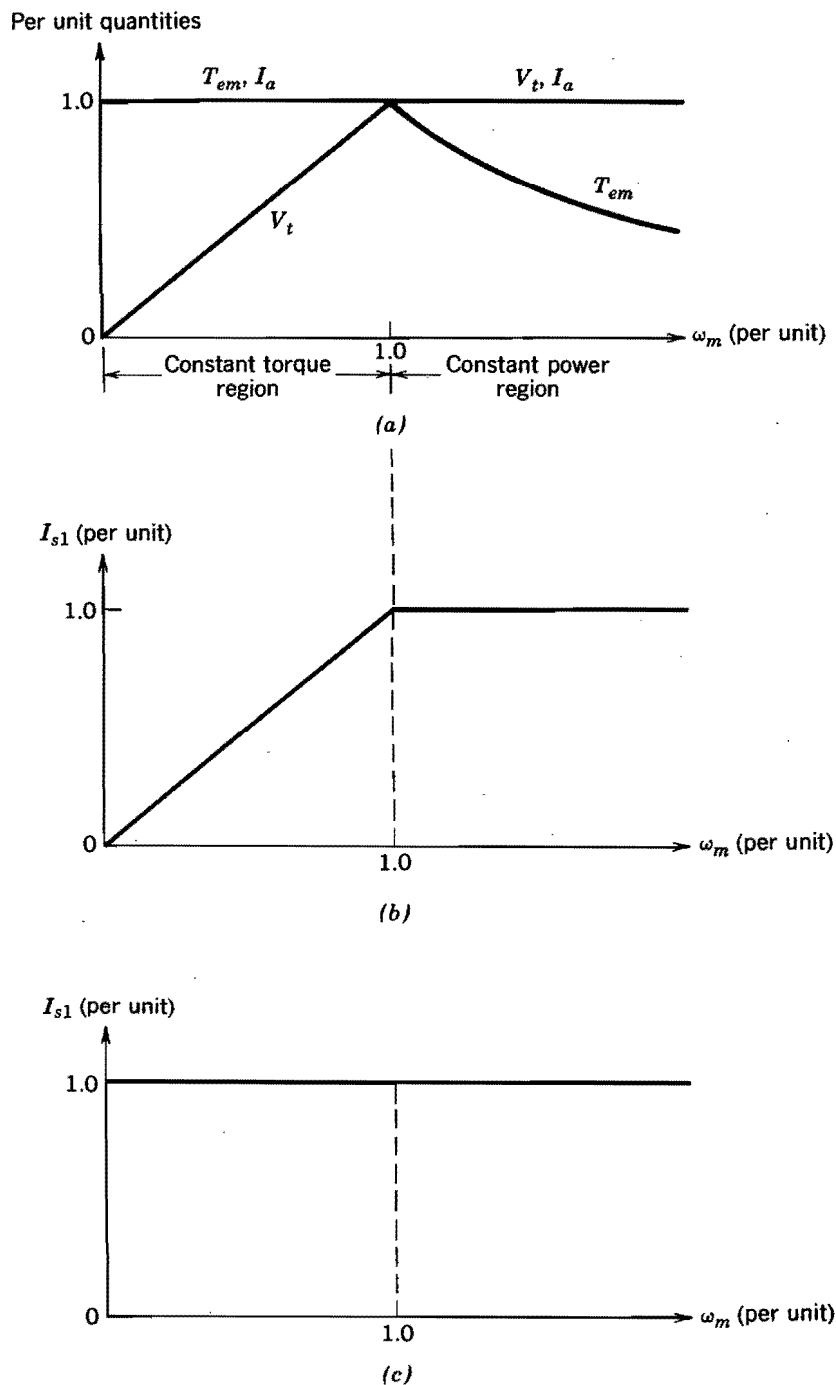


Figure 13-18 Open-loop speed control.

### 13-7-6 POWER FACTOR OF THE LINE CURRENT IN ADJUSTABLE-SPEED DRIVES

The motor operation at its torque limit is shown in Fig. 13-19a in the constant-torque region below the rated speed and in the field-weakening region above the rated speed. In a switch-mode drive, which consists of a diode rectifier bridge and a PWM dc-dc converter, the fundamental-frequency component  $I_{s1}$  of the line current as a function of speed is shown in Fig. 13-19b. Figure 13-19c shows  $I_{s1}$  for a line-frequency phase-controlled thyristor drive. Assuming the load torque to be constant,  $I_{s1}$  decreases with



**Figure 13-19** Line current in adjustable-speed dc drives: (a) drive capability; (b) switch-mode converter drive; (c) line-frequency thyristor converter drive.

decreasing speed in a switch-mode drive. Therefore, the switch-mode drive results in a good displacement power factor. On the other hand, in a phase-controlled thyristor drive,  $I_{s1}$  remains essentially constant as speed decreases, thus resulting in a very poor displacement power factor at low speeds.

As discussed in Chapters 5 and 6, both the diode rectifiers and the phase-controlled rectifiers draw line currents that consist of large harmonics in addition to the fundamental. These harmonics cause the power factor of operation to be poor in both types of drives. The circuits described in Chapter 18 can be used to remedy the harmonics problem in the switch-mode drives, thus resulting in a high power factor of operation.

## SUMMARY

1. Because of mechanical contact between the commutator segments and brushes, dc motors require periodic maintenance. Because of arcing between these two surfaces, dc motors are not suitable for certain environments.
2. In a dc motor, the field flux is established by either a field winding supplied through a dc current or permanent magnets located on the stator. The magnitude of the electromagnetic torque is directly proportional to the field flux and the armature current magnitude. This makes a dc motor ideal for servo drive applications.
3. The induced back-emf across the armature-winding terminals is directly proportional to the field flux magnitude and the rotational speed of the rotor.
4. A simple transfer function model can be obtained for a dc motor to obtain its dynamic performance.
5. The form factor of the armature current is defined as the ratio of its rms value to its average value. A poor armature current waveform with a high form factor results in excessive armature heating, arcing across commutator segments and brushes, and large torque pulsations. Therefore, an appropriate remedial action should be taken to avoid damage to the dc motor.
6. The dc motor drives utilize either the line-frequency controlled converters or the dc-dc switch-mode converters. By field weakening in a wound-field dc motor, the speed can be controlled beyond its rated value, without exceeding the rated armature voltage.
7. The power factor at which a dc motor drive operates from the utility grid and the current harmonics injected into the utility grid depend on the type of converter used: line-frequency controlled converter or switch-mode dc-dc converter.

## PROBLEMS

13-1 Consider a permanent-magnet dc servo motor with the following parameters:

$$\begin{aligned}
 T_{\text{rated}} &= 10 \text{ N-m} \\
 n_{\text{rated}} &= 3700 \text{ rpm} \\
 k_T &= 0.5 \text{ N-m/A} \\
 k_E &= 53 \text{ V/1000 rpm} \\
 R_a &= 0.37 \Omega \\
 \tau_e &= 4.05 \text{ ms} \\
 \tau_m &= 11.7 \text{ ms}
 \end{aligned}$$

Calculate the terminal voltage  $V_t$  in steady state if the motor is required to deliver a torque of 5 N-m at a speed of 1500 rpm.

- 13-2  $G_1(s) = [\omega_m(s)/V_t(s)]$  is the transfer function of an unloaded and uncontrolled dc motor. Express  $G_1(s)$  given by Eq. 13-27 in the following form:

$$G_1(s) = \frac{1/k_E}{1 + 2sD/\omega_n + s^2/\omega_n^2}$$

Calculate  $D$  and  $\omega_n$  for the servomotor parameters given in Problem 13-1. Plot the magnitude and the phase of  $G_1(s)$  by means of a Bode plot.

- 13-3 Using the servomotor parameters given in Problem 13-1, calculate and plot the change in  $\omega_m$  as a function of time for a step increase of 10 V in the terminal voltage of that uncontrolled, unloaded servomotor.
- 13-4 The servomotor of Problem 13-1 is driven by a full-bridge dc–dc converter operating from a 200-V dc bus. Calculate the peak-to-peak ripple in the motor current if a PWM bipolar voltage-switching scheme is used. The motor is delivering a torque of 5 N-m at a speed of 1500 rpm. The switching frequency is 20 kHz.
- 13-5 Repeat Problem 13-4 if a unipolar voltage-switching scheme is used.
- 13-6 In the servo drive of Problem 13-1, a PI regulator is used in the speed loop to obtain a transfer function of the following form in Fig. P13-6:

$$F_{\omega}(s) = \frac{\omega(s)}{\omega^*(s)} = \frac{1}{1 + s(2D/\omega_n) + s^2/\omega_n^2}$$

where  $D = 0.5$  and  $\omega_n = 300$  rad/s.

- (a) Draw the Bode plot of the closed-loop transfer function  $F_{\theta}(s) = [\theta(s)/\theta^*(s)]$  if a gain  $k_p = 60$  is used for the proportional position regulator in Fig. P13-6.
- (b) What is the bandwidth of the above closed-loop system?

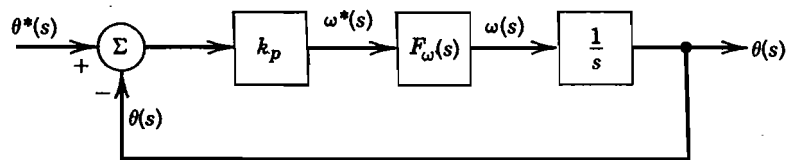
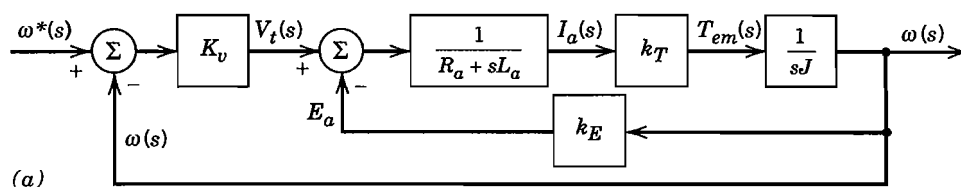
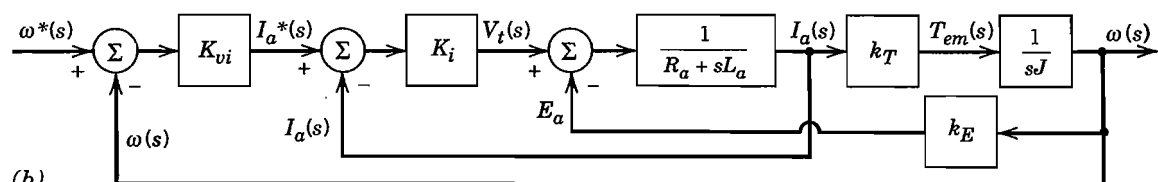


Figure P13-6

- 13-7 Consider the servomotor of Problem 13-1 in a speed-control loop. If an internal current loop is not used, the block diagram is as shown in Fig. P13-7a, where only a proportional control is used. If an internal current loop is used, the block diagram without the current limits is as shown in Fig. P13-7b, where  $\omega_n$  is 10 times that in part a.



(a)



(b)

Figure P13-7

Design the controllers ( $K_v$ ,  $K_{vi}$ ,  $K_i$ ) to yield a control loop with slightly underdamped response ( $D = 0.7$ ). Compare the two control schemes in terms of bandwidth and transient performance, assuming that the current limit is not reached in either of them.

## REFERENCES

1. A. E. Fitzgerald, C. Kingsley, Jr., and S. D. Umans, *Electric Machinery*, 4th ed., McGraw-Hill, New York, 1983.
2. P. C. Sen, *Thyristor DC Drives*, Wiley, New York, 1981.
3. G. R. Slemon and A. Straughen, *Electric Machines*, Addison-Wesley, Reading, MA, 1980.
4. T. Kenjo and S. Nagamori, *Permanent-Magnet and Brushless DC Motors*, Clarendon, Oxford, 1985.
5. *DC Motors · Speed Controls · Servo System—An Engineering Handbook*, 5th ed., ElectroCraft Corporation, Hopkins, MN, 1980.